

1 **Tau modulates mRNA transcription, alternative**
2 **polyadenylation profiles of hnRNPs, chromatin remodeling**
3 **and spliceosome complexes**

4
5 **Montalbano Mauro^{1,2}, Elizabeth Jaworski³, Stephanie Garcia^{1,2}, Anna Ellsworth^{1,2},**
6 **Salome McAllen^{1,2}, Andrew Routh^{3,4} and Rakez Kayed^{1,2†}.**

7
8 ¹ Mitchell Center for Neurodegenerative Diseases, University of Texas Medical Branch, Galveston, Texas,
9 77555, USA

10 ² Departments of Neurology, Neuroscience and Cell Biology, University of Texas Medical Branch,
11 Galveston, Texas, 77555, USA

12 ³ Department of Biochemistry and Molecular Biology, University of Texas Medical Branch, Galveston, Texas
13 77555, USA

14 ⁴ Sealy Center for Structural Biology and Molecular Biophysics, University of Texas Medical Branch,
15 Galveston, TX, USA

16 † To whom correspondence should be addressed

17

18 **Corresponding Author**

19 Rakez Kayed, PhD

20 University of Texas Medical Branch

21 Medical Research Building Room 10.138C

22 301 University Blvd

23 Galveston, TX 77555-1045

24 Phone: 409.772.0138

25 Fax: 409.747.0015

26 e-mail: rakayed@utmb.edu

27

28 **Running Title:** Tau modulates transcription and alternative polyadenylation processes

29

30 **Keywords:** Tau, Transcriptomic, Alternative Polyadenylation, Nuclear Dysfunction,
31 Neurodegeneration

32

33 **Conflict of Interest: None**

34

35 **Abbreviations:** AD, Alzheimer's disease; APA, alternative polyadenylation; DDR, DNA damage
36 response; FTD, frontal temporal dementia; GO, Gene Ontology; GSEA, gene set enrichment
37 analysis; GWAS, genome wide association study; MTs, microtubules; PAC, poly(A) cluster; PAC-
38 Seq; Poly(A)-ClickSeq, PAP, poly-A polymerase; PAS, poly(A) site; RNA, ribonucleotide acid; Tet,
39 Tetracycline; 3'UTR, 3' untranslated region; iHEK, inducible human embryonic kidney cells; ER,
40 endoplasmic reticulum;

41

42

43

44

45

46 **Author summary**

47 While tau biology has been extensively studied and closely linked to several neurodegenerative
48 diseases, our current understanding of tau's functions in the nucleus is limited. Given the role of
49 tau in disease progression and pathogenesis, elucidating the function of tau activity in
50 transcription and its nuclear accumulation may reveal novel therapeutic targets; therefore, helping
51 identify new upstream pathways that have yet to be investigated. In this study, we used tau-
52 inducible cell lines to uncover new molecular mechanisms by which tau functions in the nucleus.
53 This study systematically investigates the changes in transcriptomic and alternative
54 polyadenylation profiles modulated by WT and mutant P301L tau protein. In this manuscript, we
55 report following new findings (i) tau modulates gene expression of transcripts associated with
56 chromatin remodeling and splicing complexes; (ii) WT and mutant P301L tau regulate,
57 differentially, transcription and alternative polyadenylation (APA) profiles; and (iii) P301L mutation
58 affects the transcription mediated by tau protein. The potential role of tau in mediating
59 transcription and alternative polyadenylation processes is not well studied, representing a novelty
60 in the field. Therefore, this research establishes a new direction for investigating tau nuclear
61 function in both human and mouse brains.

62
63
64
65
66
67
68
69
70
71
72
73
74
75
76
77
78

79 **Abstract**

80

81 Tau protein is a known contributor in several neurodegenerative diseases, including Alzheimer 's

82 disease (AD) and frontotemporal dementia (FTD). It is well-established that tau forms pathological

83 aggregates and fibrils in these diseases. Tau has been observed within the nuclei of neurons, but

84 there is a gap in understanding regarding the mechanism by which tau modulates transcription.

85 We are interested in the P301L mutation of tau, which has been associated with FTD and

86 increased tau aggregation. Our study utilized tau-inducible HEK (iHEK) cells to reveal that WT

87 and P301L tau distinctively alter the transcription and alternative polyadenylation (APA) profiles

88 of numerous nuclear precursors mRNAs, which then translate to form proteins involved in

89 chromatin remodeling and splicing. We isolated total mRNA before and after over-expressing tau

90 and then performed Poly(A)-ClickSeq (PAC-Seq) to characterize mRNA expression and APA

91 profiles. We characterized changes in Gene Ontology (GO) pathways using EnrichR and Gene

92 Set Enrichment Analysis (GSEA). We observed that P301L tau up-regulates genes associated

93 with reactive oxygen species responsiveness as well as genes involved in dendrite, microtubule,

94 and nuclear body/speckle formation. The number of genes regulated by WT tau is greater than

95 the mutant form, which indicates that the P301L mutation causes loss-of-function at the

96 transcriptional level. WT tau up-regulates genes contributing to cytoskeleton-dependent

97 intracellular transport, microglial activation, microtubule and nuclear chromatin organization,

98 formation of nuclear bodies and speckles. Interestingly, both WT and P301L tau commonly down-

99 regulate genes responsible for ubiquitin-proteasome system. In addition, WT tau significantly

100 down-regulates several genes implicated in chromatin remodeling and nucleosome organization.

101 Although there are limitations inherent to the model systems used, this study will improve

102 understanding regarding the nuclear impact of tau at the transcriptional and post-transcriptional

103 level. This study also illustrates the potential impact of P301L tau on the human brain genome

104 during early phases of pathogenesis.

105

106 **Introduction**

107 Tau is a neuronal protein found both inside and outside of the nucleus that contributes to the
108 pathology of neurodegenerative diseases such as frontotemporal dementia (FTD) and
109 Alzheimer's disease (AD)¹. It is primarily described as a microtubule-associated protein². Nuclear
110 tau has been found to 'protect' DNA¹⁻³ during reactive oxygen species (ROS)-induced heat stress.
111 However, nuclear and cytosolic tau interact with RNA to form droplets⁴ and aggregates⁵. Tau has
112 also been observed altering nuclear structure^{6,7} in the human nuclei of neuroblastoma^{8,9} and in
113 HEK-293 cells. More specifically, phosphorylation of nuclear tau negatively regulates its nuclear
114 function in pluripotent neuronal cells and neuroblastoma cells¹⁰. Previous studies have revealed
115 that nuclear tau plays a role in the DNA damage response (DDR) through deadenylation, which
116 triggers major mRNA decay pathways^{11,12}. Most recently, we found that oligomeric assemblies of
117 tau containing RNA-binding proteins impair chromatin remodeling and nuclear lamina formation
118 through associations with histones and chromatin components in the nuclear compartment¹³.

119 Despite the well-established importance of tau in the cytoskeleton of neurons¹⁴, there is
120 growing evidence that tau is notably involved in nucleolar transcription and cellular stress
121 responses^{15,16}. Recently, it was shown that mutations and/or the phosphorylation of tau results in
122 the deformation of the neuronal nuclear membrane and can disrupt nucleocytoplasmic transport¹⁷
123 in FTD^{7,18} and AD^{19,20}. Related studies analyzed the direct impact in transcriptional activity due to
124 tau and found that nuclear tau regulates the expression of VGluT1, a gene that controls
125 glutamatergic synaptic transmission, and that tau displacement from microtubules (MTs)
126 increases nuclear accumulation of tau²¹. Furthermore, tau modifies histone acetylation and was
127 shown to have a broad epigenomic impact in the aging and pathology of AD human brains²². It
128 has also been observed that tau interacts with neuronal pericentromeric DNA regions, particularly
129 in association with HP1 and H3K9me3²³, this observation spots tau protein as potential chromatin
130 remodeling factor. Lastly, tau exhibits binding interactions with genic and intergenic DNA

131 sequences of primary cultured neurons, especially in positions ± 5000 bp away from the start site
132 of transcription²⁴.

133 In eukaryotic cells, the maturation of 3' ends in mRNA involves endonucleolytic cleavage
134 of the nascent RNA followed by the synthesis of a poly(A) tail on the 3' terminus of the cleaved
135 product by a poly(A) polymerase (PAP)²⁵. This reaction is called polyadenylation and is
136 fundamentally linked to transcription termination. The sequences for the mRNA precursors and
137 the proteins required for polyadenylation are well understood. It has been clearly elucidated that
138 a single gene can give rise to many possible transcripts, each with different polyadenylation sites
139 (poly(A)-sites, or PASs), and that differential usage of these sites can lead to the formation of
140 mRNA isoforms. This phenomenon is called alternative polyadenylation (APA)²⁶ and is a common
141 event in eukaryotic cells. In fact, researchers have determined that 50% of mammalian mRNA-
142 encoding genes express APA isoforms^{27,28}. Considering this information, we used tau inducible
143 HEK (iHEK) cell lines to obtain and analyze transcriptomic and APA profiles in the presence of
144 WT and P301L tau. To characterize transcriptional and post-transcriptional profiles modified by
145 WT and P301L, we utilized Poly(A)-ClickSeq (PAC-Seq) to measure changes in the expression
146 of the host mRNA transcript whilst simultaneously characterizing changes in the PAS usage or
147 creation of mRNA isoforms. In addition, we employed Gene Set Enrichment Analysis (GSEA) and
148 Gene Ontology (GO) to study the main gene domains modulated by tau.

149

150

151

152

153

154

155

156 **Materials and Methods**

157 **Cell Culture and Tau Expression.** In this study we used two different versions of tau inducible
158 HEK (iHEK) cells: iHEK overexpressing WT tau and iHEK overexpressing mutated P301L tau.
159 They were maintained in Dulbecco's modified eagle medium (DMEM) supplemented with 10%
160 fetal bovine serum (FBS) at 37 °C in 5% CO₂. To induce WT and mutant tau overexpression,
161 iHEK cells were treated with 1µg/mL of Tetracycline (Tet) for 24 hours in FBS-depleted DMEM
162 (Gibco™ LS11965118, Fisher Scientific). iHEK cells not treated with Tet were named control (Ctr).
163 After 24 hours, two washes with medium were done to remove excess Tet. Immediately after the
164 washes, the cells were stained and collected. Detachment of cells was completed with Trypsin
165 (Gibco™ Trypsin-EDTA, 0.25% Phenol red, LS25200114 Fisher Scientific), and the cells warmed
166 for 3 minutes in the incubator following the addition of Trypsin. The cells were then centrifuged at
167 1000 rpm for 5 minutes. Lastly, cell pellets were harvested and used for protein fractionation, and
168 mRNA extraction.

169
170 **RNA Extraction.** Total mRNA was collected by using TRIzol extraction reagent according to
171 established protocol²⁹. RNA samples for Real Time Analysis (RT-PCR) were quantified using a
172 Nanodrop Spectrophotometer (Nanodrop Technologies), followed by analysis on an RNA Nano
173 chip using the Agilent 2100 Bioanalyzer (Agilent Technologies). Only samples with high quality
174 total RNA were used (RIN: 7.5-10.0) for the study. Synthesis of cDNA was performed with either
175 0.5µg or 1µg of total RNA in a 20µl reaction using the reagents available within the Taqman
176 Reverse Transcription Reagents Kit from Life Technologies (#N8080234). Q-PCR amplifications
177 (performed in duplicate or triplicate) were done using 1µl of cDNA in a total volume of 20µl using
178 the iTaq Universal SYBR Green Supermix (Bio-Rad #1725125). The final concentrations of the
179 primers were 300nM. Relative RT-QPCR assays are performed with either 18S RNA gene as a
180 normalizer. Absolute RNA quantification analysis was performed using known amounts of a
181 synthetic transcript created from the gene of interest.

182

183 **Library Preparation Protocol.** Protocols for Poly(A)-ClickSeq (PAC-Seq) have been described
184 in detail by Jaworski et al. 2018^{30,31}. Approximately 1µg of total cellular RNA per sample was used
185 as a template in reverse-transcription reactions supplemented with 40uM Azido-VTPs and primed
186 using an oligo-dT primer containing a partial Illumina i7 indexing adaptor. Azido-terminated cDNA
187 fragments were 'click-ligated' to hexynyl-functionalized click-adaptors containing the Illumina i5
188 universal sequencing adaptor. Single-stranded cDNA libraries were indexed in a final PCR
189 reaction for 15-18 PCR cycles. Final libraries were size extracted by gel-electrophoresis and
190 submitted for sequencing using an Illumina NextSeq550 to prepare 1x150 SE reads. RNAseq
191 datasets is uploaded to NCBI SRA, reference number: [PRJNA744518](#).

192

193 **Poly(A)-ClickSeq.** PAC-Seq data were analyzed using the Differential Poly-A Clustering (*DPAC*)
194 program, which ran with default settings as previously described³². *DPAC* trims and quality-filters
195 raw FASTQ data and therefore requires each read to have at least 25 'As' at the 3' end of the
196 read. These reads are then trimmed using *cutadapt*. Trimmed reads are mapped to the reference
197 human genome (hg19) using *HISAT2*³³. The 3'end of mapped reads are thus used to annotate
198 poly(A)-sites and annotated based upon overlaps with gene annotations obtained from UCSC
199 genome browser. Gene counts were extracted and *DESeq2* was used to calculate changes in
200 gene expression as well as relative changes in expression in individual poly(A)-sites found within
201 single genes. Differential gene expression was assigned when a gene had a fold change greater
202 than +/- 1.5-fold with a p-adj value less than 0.1. Alternative polyadenylation is assigned when a
203 single gene has two or more clustered poly(A)-sites wherein at least one of these sites has a
204 differential usage greater than a +/- 1.5-fold, a p-adj value less than 0.1, and a change of the
205 relative usage of a poly(A)-cluster within the gene of greater than 10%.

206

207 **Western Blotting and Cell Fractioning.** Immunoblot (IB) analyses were performed with iHEK
208 cell fraction samples as previously described¹³. Approximately 10 µg of protein preparations were
209 loaded onto precast NuPAGE 4-12% Bis-Tris gels (NP0335BOX, Invitrogen) for sodium dodecyl
210 sulfate-polyacrylamide gel electrophoresis (SDS-PAGE) analyses. Gels were subsequently
211 transferred onto nitrocellulose membranes and blocked overnight at 4°C with 10% nonfat dry milk.
212 Membranes were then probed for 1 hour at room temperature with Pan-Tau (Tau13, 1:10,000,
213 MMS-520R Covance), (GAPDH, 1:1000, ab9485 Abcam), Histone3 (1:1000, ab201456 Abcam),
214 RCC1 (1:100, Clone E-6 sc-55559 Santa Cruz Tech.), DNAJC2 (1:5000, ab134572 Abcam),
215 Histone 1.2 (1:500, ab4086 Abcam), HMGB1 (1:500, ab18256 Abcam), SMARCA5 (1:10000,
216 #PA5-78253, Invitrogen), SMARCC1 (0.4µg/mL, #PA5-55058, Invitrogen), and β-Actin (1:5000,
217 #A1978, Sigma Aldrich). Antibodies were diluted in 5% nonfat dry milk. Immunoreactivity was
218 detected using a horseradish peroxidase (HRP)-conjugated anti-rabbit immunoglobulin G (IgG,
219 1:10,000, NA934 GE Healthcare). Tau13 and Tau5 immunoreactivity were detected using an anti-
220 mouse IgG (1:10,000, NA931 GE Healthcare) diluted in 5% milk. ECL Plus (K-12045-D50, GE
221 Healthcare) was used to visualize protein bands. LaminB1/Histone3 and GAPDH were used to
222 normalize and quantify nuclear and cytoplasmic proteins, respectively. The compartment
223 extraction was conducted with Qproteome Cell Compartment Kits (Qiagen, #37502); nuclear, cell
224 membrane, and cytoplasmic proteins were isolated and preserved for IB analysis.

225 **Immunofluorescence of Fixed Cells and Fluorescence Microscopy.** Cells on a 24-well
226 coverslip were fixed with 0.5 ml of 4% PFA/PBS for 15 min. The cells were then washed 3 times
227 in phosphate buffered saline (PBS), for 5 min for each wash. The cells were permeabilized in
228 0.5ml PBS and 0.2% Triton X-100 in phosphate buffered saline containing 0.5% Tween (PBST)
229 for 5 min. Blocking was done in 0.5 ml of 5% normal goat serum (NGS) in PBST for 1 hour.
230 Primary antibody was diluted in 5% NGS/PBST overnight at 4°C for incubation, and then washed
231 3 times in PBST, for 10 min each. Secondary antibody diluted in 5% NGS/PBST was incubated

232 for 2 hours at room temperature. All the secondary antibodies were purchased from Thermo
233 Fisher Scientific and used at a 1:800 dilution for staining. After applying secondary antibodies,
234 cells were incubated in DAPI (nuclei staining) diluted 1:10,000 in PBST (5 mg/ml stock solution)
235 for 5 min after the first wash. The cells were then washed 2 times with PBST, and once with PBS
236 (10 min each) prior to mounting coverslips. Coverslips were mounted on glass microscope slides
237 using 8-10 μ l of Prolong Gold Antifade mounting media with DAPI (Invitrogen, P36941) per
238 coverslip. Slides were air-dried in fume hood or stored at 4°C until ready to be dried in the fume
239 hood. The primary antibodies used in this study for immunocytochemistry (ICC) are as follows:
240 Histone 1.2 (Abcam ab4086 - 1 μ g/ml), Ki-67 (Abcam ab92742 - 1 μ g/ml), SMARCC1 (Invitrogen
241 PA5-55058 - 0.25 μ g/ml, SMARCA5 (Invitrogen PA5-78253 - 1 μ g/ml, MCM2 (Abcam ab108935
242 - 1/1000), RCC1 (Santa Cruz, INC. sc-55559 - 1:50), and Tau13 (Bio Legend MMS-520R - 1/200).
243 After three washes with PBS, cells were probed with mouse and rabbit-specific fluorescent-
244 labeled secondary antibodies (1:200, Alexa Fluor 488 and 633, Life Technologies). Single frame
245 images were collected using the Keyence BZ-X 710 Microscope. Images for quantification of area
246 and integrated density were taken in nuclear target areas guided by the DAPI fluorescence. We
247 then performed single extraction analysis using BZ-X Analyzer software (Keyence). We used 200
248 nuclei per target area and used the Nikon 20X objective for imaging and quantification analysis.

249

250 **Statistical Analysis.** All in-vitro experiments were performed in at least three biological
251 replicates. All data are presented as means \pm SD and were analyzed using GraphPad Prism
252 Software 6.0. Statistical analyses included the Student-t Test or one-way ANOVA followed by
253 Tukey's Multiple Comparisons Test. Column means were compared using one-way ANOVA with
254 treatment as the independent variable. In addition, group means were compared using two-way
255 ANOVA considering factors for each treatment respectively. When ANOVA showed a significant
256 difference, pair-wise comparisons between group means were examined by the Tukey and
257 Dunnett Multiple Comparison Test.

258

259 **Results**

260 **WT tau up-regulates genes associated with cytoskeleton organization and nuclear**
261 **speckles/bodies.** Firstly, we evaluated changes in gene expression profiles upon expression of
262 WT and P301L tau in iHEK cells that were induced with tetracycline (Tet). After 24h of Tet
263 induction, we confirmed tau expression in the cytoplasm and nuclei of iHEK cells (Fig S1A). Total
264 cellular RNA from WT and P301L tau (untreated (Control) and treated (+Tet)) study groups was
265 extracted using TRIzol reagent and by following established protocol^{7,13}. RNA was sequenced
266 using Poly(A)-ClickSeq (PAC-Seq) to measure changes in gene expression and poly(A)-site
267 usage³¹. A schematic of the experimental design is provided in Fig 1A. Volcano scatterplots from
268 WT and P301L tau iHEK (Fig 1B and 1C, respectively) demonstrate a substantial difference in
269 the number of genes regulated by WT tau and P301L tau. After Tet induction in the WT tau iHEK
270 cell system, we observed up-regulation of 88 genes and down-regulation of 30 genes (gene
271 names listed in Fig 1D). In the P301L tau iHEK cell system, these numbers dropped to 10 up-
272 regulated genes and only 1 down-regulated (gene names listed in Fig 1E).

273 Fig S1B displays the scatterplots of WT and P301L tau gene expression, while Fig S1C
274 reports the Principal Component Analysis (PCA). PCA demonstrates significant variation among
275 the study groups. More specifically, the analysis suggests a significant difference in transcriptional
276 activity of WT tau due to the higher number of genes modulated in comparison to the mutant
277 P301L tau form. Using EnrichR³⁴, we established Gene Ontology (GO) of the biological processes,
278 molecular functions, and cellular components altered by both the up-regulated and the down-
279 regulated sets of genes. WT tau GO is summarized in Fig 2. WT tau up-regulated genes belonging
280 mainly to classes of cytoskeleton-dependent intracellular transport genes (GO: 0030705,
281 TUBA1A, TUBB2B TUBA1B, TUBB2A and HOOK3) and genes responsible for the regulation of
282 cytoskeleton organization (GO: 0051493). Imbalanced expression of tubulin and tau induces

283 neuronal dysfunction in *C. elegans*,³⁵ indicating that tau itself can disturb tubulin gene expression.
284 The reason behind this pronounced involvement of TUBB genes could be due to the fact that
285 *TUBB1B*, *TUBB2B*, *TUBA1A* and *TUBB2A* are clustered together within the genome³⁶.

286 It is important to note that biological process such as microglial cell activation (GO:
287 0001774) and macrophage activation (GO: 0042116) were also observed as being up-regulated,
288 which confirms known effects of tau on the neuro-inflammatory response commonly observed in
289 neurodegenerative diseases³⁷. Neuro-immunomodulation can also effect cytoskeleton
290 reorganization³⁸. Our GO analysis revealed up-regulated genes involved in mitochondrion
291 distribution (GO: 0048311, *MAPT* and *MEF2A* genes), morphogenesis (GO: 0070584, *SUPV3L1*
292 p=0.03892), neurogenesis (GO 0022008, *NOM1*, *MAPT* and *DAGLB* genes), and positive
293 regulation of cell death (GO 0010942, *SAP30BP*, *MAPT* and *CLU* genes). The increase of *CLU*
294 expression was a particularly interesting observation. Clusterin is a multifunctional, secreted
295 chaperone involved in several basic biological events, including cell death, tumor progression and
296 neurodegeneration. The *CLU* gene is notably associated with an increased AD risk³⁹. In terms of
297 molecular functions, the up-regulated genes we observed have several enriched pathways,
298 including RNA binding (GO: 0003723, *USP36*, *NOM1*, *TFRC*, *BAZ2A*, *SUPTSH*, *PHF6*, *FTSJ3*,
299 *SUPV3L1*, *TUBA1B*, *RBM20*, *MAPT*, *RBM33*, *PELP1*, *HIST1H1C*, *CPEB4*) and several nuclear
300 functions, such as histone deacetylase binding (GO: 0042826, *MEF2A*, *SUDS3* and *PHF6*) and
301 sequence-specific double stranded DNA binding (GO: 1990837, *MEF2A*, *KAT7* and *MAPT*).

302 Transcriptional products of up-regulated genes are mostly localized in the cytoplasm and
303 nuclear compartments. We detected transcripts associated with nuclear chromatin (GO:
304 0000790), such as *MEF2A*, *ZEB2*, *ANP32E*, *SUDS3*, *HIST2H2AC*, and *HIST1H1C*. We also
305 examined nuclear speck transcripts (GO: 0016607), such as *CARMIL1*, *USP36*, *GTF2H2C*,
306 *BAZ2A*, and *MAPT* genes, which are also included in nuclear body components (GO: 0016604),
307 along with *SUDS3* and *SENP2*. The other cell compartment well represented in our GO analysis

308 is the cytoplasm. In particular, the microtubule cytoskeleton (GO: 0015630) contained the
309 following up-regulated genes: *TUBB2B*, *SAP30BP*, *TUBA1B*, *TUBA1A*, *TMOD3*, *MAP7*, *TARS*,
310 *TACC1*, *MAPT*, *CLU*, and *RHOQ*. A complete Enrich-GO list of significant up-regulated genes
311 observed in WT tau is presented in Supplemental Table 1.

312

313 **WT tau down-regulates genes involved in ubiquitin-related processes as well as**
314 **genes associated with Golgi and mitochondrial components.** Overall, thirty genes were
315 significantly downregulated by WT tau protein. The main biological process affected was the
316 regulation of cellular component organization (GO: 0051128) as it relates to cytoskeleton
317 organization and structure morphogenesis. Molecular functions associated with the
318 aforementioned genes are closely related to ubiquitin protein ligase binding (GO: 0031625) and
319 ubiquitin-like protein ligase binding (GO: 0044389). Genes important to neuronal components
320 included genes essential to the structure of initial axonal segments, nodes of Ranvier, and main
321 axons. These three groups typically involve the gene *KCNQ2*. This gene encodes for Potassium
322 voltage-gated channel subfamily KQT member 2, which plays a critical role in determining the
323 subthreshold electrical excitability of neurons as well as the responsiveness of neurons to
324 synaptic inputs. Therefore, *KCNQ2* is important in the regulation of neuronal excitability and the
325 loss-of-function or gain-of function of this gene can lead to various forms of neonatal epilepsy⁴⁰.

326 Furthermore, Cullin-RING E3 ubiquitin-ligase complex component *KLHL11* is down-
327 regulated, as well as the *STX6* gene. *STX6* encodes for Syntaxin-6, which is involved in
328 intracellular vesicle trafficking and is integrally associated with the Golgi apparatus. Another Golgi
329 protein that is down-regulated is Golgin-45 (*BLZF1*). It is required for normal Golgi structure and
330 for protein transport from the Endoplasmic Reticulum (ER) through the Golgi apparatus to the cell
331 surface⁴¹. Lastly, the ER gene *STC2* is downregulated and encodes for Stanniocalcin-2. This
332 glycoprotein has an anti-hypocalcemic action on calcium and phosphate homeostasis⁴².

333 We also detected two nucleolus-localized genes among the down-regulated group:
334 UBE2T (ubiquitin-conjugating enzyme with E2 T) and UPF3A, (a regulator of nonsense transcript
335 3A). The mitochondrial genes that were down-regulated included OXCT1 (Succinyl-CoA: 3-
336 ketoacid coenzyme A transferase 1, mitochondrial enzyme), TRUB1 and PFDN2 (Prefoldin
337 subunit 2). An Enrich-GO list of downregulated genes present in WT tau is depicted in
338 Supplemental Table 2.

339 Although there are limitations inherent with the model used, these data suggest that WT
340 tau intrinsically and significantly impacts the cell at a transcriptional level. More specifically, a
341 higher number of genes are up-regulated and down-regulated by WT tau when compared to
342 P301L tau. This suggests that the P301L mutation leads to a loss-of-function (LOF) of tau at the
343 transcriptional level. This sort of loss could have detrimental effects on cell structure and
344 organization.

345
346 **P301L tau up-regulates gene expression of components related to axonal microtubule**
347 **skeleton, nuclear speckles, and ribonucleoprotein.** The GO pathways and cellular
348 compartments upregulated and downregulated by P301L tau are listed In Supplemental Tables 3
349 and 4 respectively. As observed in WT tau iHEK cells, the *MAPT* gene is on the upregulated
350 gene list for P301L tau, as expected after Tet induction of the iHEK cells. Within the group of
351 axonal and cytoskeleton genes, we noticed up-regulation of NLGN1, a gene that encodes for
352 Neuroligin-1. Neuroligin is a postsynaptic neuronal surface protein involved in cell-to-cell
353 interactions via its interactions with neurexin family members⁴³. It has been established that the
354 NLGN1 gene is associated with amyloid- β oligomers (A β O) in AD-causing synaptic impairment⁴⁴.
355 In addition, NLGN1 is typically altered in AD hippocampi and also modulates amyloid-beta
356 oligomer toxicity⁴⁵. Neuroligin-1 plays an influential role in synaptic function and synaptic signal
357 transmission, most likely through its ability to recruit and cluster together other synaptic proteins⁴³.

358 For instance, neuroligin-1 may promote the initial formation of synapses⁴⁶, but is not essential for
359 the complete formation of synapses. *In vitro*, Neuroligin-1 triggers the *de novo* formation of
360 presynaptic structures. NLGN1 may also be involved in specification of excitatory synapses⁴³. For
361 example, NLGN1 functions to maintain wakefulness quality and normal synchrony of cerebral
362 cortex activity during wakefulness and sleep⁴⁷. Neuroligin-1 is predominantly located in synaptic
363 cleft of the cell membrane⁴⁸.

364 When we analyzed upregulated genes, we detected a considerable number of genes
365 related to nuclear body (GO: 0016604) and nuclear speck (GO:0016607) domains including the
366 genes *ITPKC* and *MAPT*. Interestingly, it has been observed that the *FER* gene participates in
367 several different cytoplasmic and nuclear functions. For example, *FER* is associated with nuclear
368 chromatin (GO:0000790) and the microtubule skeleton (GO:0015630). The *FER* gene also
369 encodes for a tyrosine-protein kinase that plays a role in synapse organization, trafficking of
370 synaptic vesicles, the generation of excitatory post-synaptic currents, and neuron-to-neuron
371 synaptic transmission⁴⁹. Lastly, *FER* plays a role in neuronal cell death after brain damage⁴⁹. The
372 only gene down-regulated by P301L tau is *DCAF12*, which is a component of the Cullin-RING
373 ubiquitin ligase complex⁵⁰. This gene is also down-regulated by WT tau and belongs to genes
374 associated with ubiquitination processes. The failure of ubiquitination pathways is known to
375 have a strong connection to neurodegenerative diseases⁵¹. Supplemental Figure 2 summarizes
376 upregulated and downregulated genes in P301L tau, subcategorized by biological process and
377 molecular function.

378 In summary, the P301L mutation upregulates genes involved in positive regulation of
379 neuronal death and responsiveness to reactive oxygen species (ROS) production. This is in contrast
380 to the genes altered by WT tau that have a greater effect on cell structural processes. The most
381 important molecular function altered by such genes would be sequence-specific double-stranded
382 DNA binding, transcriptional expression, and chromatin remodelling. Overall, our GO data

383 suggests the presence of both loss-of-function (LOF) and gain-of-function (GOF) events in
384 mutated P301L tau that may relate to pathology. Modulating genes known to be associated with
385 neurodegenerative disease suggests that mutated tau engenders harmful transcription patterns
386 that contribute to the well-established effects of tau proteinaceous-aggregation toxicity.

387

388 **WT tau modulates gene expression of chromatin organization and remodeling factors.**

389 Gene Set Enrichment Analysis (GSEA) offers an opportunity to evaluate and identify classes of
390 genes or proteins that are over-represented in a large set of genes or proteins and may have an
391 association with disease phenotypes. Due to the differences in gene numbers modulated by WT
392 tau versus P301L tau, we performed GSEA. This analysis compared models with and without WT
393 tau. We observed that WT tau down-regulates the expression of numerous genes linked to
394 chromatin organization (Fig 3A) and chromatin remodeling (Fig 3B) domains. By looking at the
395 chromatin organization and remodeling gene clusters, we identified that several high-mobility
396 group box proteins (HMG) *HMGN5*, *HMGB2* and *HMGA1* are up-regulated while *HMGB1* and
397 *HMGN1* are down-regulated. It is important to note that *HMGB1* is an activator of neuro-
398 inflammatory responses and has been implicated in AD⁵². In addition, several components of the
399 SWI/SFN chromatin remodeling complex are downregulated. The identification of genes
400 *SMARCE1*, *SMARCA5* and *SMARCC1*, imply that tau has a substantial impact on chromatin
401 remodeling in the cells. The heterogeneous nuclear ribonucleoproteins (hnRNPs), *HNRNPU* and
402 *HNRNPC*, were also found to be downregulated in WT tau. Down-regulation of several factors
403 implicated in DNA replication and repair processes, indicates that WT tau also significantly affects
404 the nuclear compartment of cells in terms of structure and content. Several of these genes are
405 clustered as covalent chromatin modification in GO (Fig 3C).

406 To validate gene expression changes observed in GSEA analysis, we verified multiple
407 proteins via western blot by using the up-regulated and down-regulated lists generated from
408 Histone Binding GO. We verified up-regulation of *RCC1*, *DnaJC2* and *Histone1.2* proteins in the

409 cytoplasm and in nuclear fractions of WT and P301L tau iHEK cells (Fig 3D). We also confirmed
410 RCC1 expression and noticed its accumulation in the cytoplasm for both cell lines. Interestingly,
411 we discerned that RCC1 is not imported into the nuclei where it should function as a regulator of
412 chromatin condensation. Instead, DnaJC2 in P301L tau iHEK cells appear to be downregulated.
413 However, Histone 1.2 is upregulated in both cell lines. We did not observe down-regulation of
414 the chromatin remodeling complex factors SMARCC1 and SMARCA5. Instead, we detected their
415 accumulation in the cytoplasmic fractions while in the presence of tau, which suggests a deficit in
416 these factors in the nuclei, as observed in our western blots. Lastly, HMGB1 and β -Actin are
417 down-regulated, but HMGB1 is not detected in the nuclei when in the presence of tau. Histone 3
418 was used as a nuclear loading control.

419 To verify gene expression results, alongside western blots, we performed co-
420 immunofluorescence in WT tau iHEK cells. We evaluated integrated density of Histone 1.2 (Fig
421 3E and 3F), Ki67 (Fig 3G and 3H), SMARCC1 (Fig 3I and 3J), and SMARCA5 (Fig 3K and 3L).
422 Analysis was performed by considering nuclear integrated density of “-” and “+” tau WT iHEK
423 proteins. To detect and confirm tau expression, we used the Tau13 antibody. MCM2 and RCC1
424 images and their relative integrated density quantifications are presented in Supplemental Fig. 4.

425 GSEA analysis for WT tau revealed significant down-regulation in the pathways for
426 histone-binding (Fig 4A) and nucleosome organization clusters (Fig 4B). Several genes were
427 detected in the histone and nucleosome domains, which were recurring and can be viewed in the
428 chromatin gene list showed in Fig 3. In addition, we observed an up-regulation of *RCC1* (a
429 regulator of chromosome condensation), *CTSL* (Cathepsin L), *MCM2* (Minichromosome
430 maintenance complex component 2), and *DNAJC2* (DnaJ heat shock protein member C2). In
431 Nucleosome GO, we observed up-regulated *HMGB2* and *HMGA1* (high mobility group box B2
432 and A1). On the contrary, several Lysine acetylation regulators were downregulated: *BRD3* and
433 *BRD9* (from BRD family), *HDAC2*, *KDM5B*, *KAT7*, and *SFTD2*.

434 We also used western blotting to verify tau levels in cytoplasm and nuclear fractions of
435 WT and P301L tau iHEK cells (Fig 4C and 4D, respectively). We found that upon Tet induction in
436 both compartments, tau was detected, which was previously observed⁷ and expected. Western
437 blot analysis demonstrated that tau is represented mainly in its monomeric form (mTau_N) when
438 probing the nucleus. We compared the level of mTau_N in both cell lines and we determined that
439 mTau_N increased in both cell lines after Tet induction. However, the WT mTau_N was present in a
440 significantly higher level when compared to the P301L mTau_N (Fig 4E). This difference is due to
441 the higher *MAPT* transgene expression efficiency in WT tau iHEK cell lines as was confirmed by
442 RT-qPCR in a previous study⁷. These observations suggest that the monomeric form of tau
443 protein predominantly carries out transcriptional activity and that the P301L mutation did not affect
444 the nuclear import of tau, but instead modulated transcriptional activity. Cytoplasmic mTau was
445 quantified as well (Supplemental Figure 4). In general, we propose that WT and P301L tau both
446 shuttle into the nuclei but then modulate transcription differently. The schematic model for this
447 idea is represented in Fig 4F. In summary, many nuclear factor genes involved in several nuclear
448 activities, including chromatin condensation, are downregulated in WT tau, which indicates a
449 potential role of WT and P301L tau in the control of chromatin factors, expression and subsequent
450 cellular localization.

451

452 **RNA metabolism, chromatin organization and *HNRNPs* precursor's display shortened**
453 **APAs in the presence of WT tau.** From PAC-seq analysis, we identified 110 genes with
454 shortened 3'UTRs. The majority of these shortened genes belong to significant pathways
455 associated with mRNA processing (GO: 0006397), RNA Splicing (GO: 0000377, GO: 0000398),
456 and RNA metabolic processes (GO: 0016070) (Fig 5A). These domains share several genes:
457 *HNRNPA3*, *SRRT*, *PRPF4B*, *CCAR1*, *LSM8*; *SNRNP40*, *HNRNPK*, *ZMAT2*, *ZC3H11A*,
458 *HNRNPF*, *PCBP2*, *SNRPE*, and *HNRNPC*. The regulation of responses to DNA damage (GO:

459 2001020) comprise the following genes: *BCLAF1*, *FMR1*, *USP1* and *HMGA2* (others listed in Fig
460 5B).

461 Within the shortened APA precursors, various genes are related to nuclear function, such
462 as the chromosome related genes (GO: 0005694) *IK*, *FMR1*, *HMGA2*, *SMC4*, *SMC3*, *SMC2* and
463 *SMC6*. Structural maintenance of chromosome (SMC) proteins are ATPases that are essential to
464 chromosomal condensation, sister-chromatid cohesion, recombination, DNA repair, and
465 epigenetic silencing of gene expression⁵³. Eukaryotes have at least six genes encoding SMCs
466 (SMC1-SMC6)⁵⁴. They inherently work as heterodimers: SMC1/SMC3 (Cohesin Complex),
467 SMC2/SMC4 (Condensin Complex) and SMC5/SMC6⁵⁴.

468 Several nucleolar (GO: 0005730) genes have altered poly(A) site usage by WT tau
469 including: *PARP1*, *FMR1*, *CHD7*, *DDX21*, *PWP1*, *PPM1E*, *SMC2*, *RSL1D1*, *ILF3*, *NCL*, *S100A13*,
470 *KIF20B*, *RAN*, and *GET4*. As we saw in the shortened 3'UTRs, the most affected genes for
471 lengthened 3' UTRs lie within the RNA binding function domain (GO: 0003723). mRNA
472 processing, RNA splicing, and nucleic acid metabolic processes received the top scores,
473 indicating a strong impact of WT tau in the regulation of mRNA isoforms at different levels. All
474 significant enrichment terms are clustered and represented in a scatterplot in Fig 5C. In the mRNA
475 processing domain (GO: 0006397) we identified several heterogeneous nuclear
476 ribonucleoproteins (hnRNPs) genes (*HNRNPA3*, *HNRNPK*, *HNRNPF*, *HNRNPC*, *HNRNPDL*).
477 HnRNPs are involved in alternative splicing, transcriptional and translational regulation, stress
478 granules formation, cell cycle regulation, and axonal transport⁵⁵. Their dysfunction has been
479 shown have neurological implications, but their roles have not been comprehensively
480 investigated. Several neurodegenerative diseases, including AD, FTD, and amyotrophic lateral
481 sclerosis (ALS) have been associated with hnRNPs when it comes to the progression of these
482 pathologies⁵⁶. More specifically, hnRNPK has been linked to the transcripts of several cytoskeletal
483 genes, including *MAPT*, which is needed for axonogenesis⁵⁷.

484 In Alzheimer's disease, hnRNPC promotes APP translation⁵⁸ and stabilizes the APP
485 precursors mRNA, which could suggest that increasing hnRNPC levels may promote A β
486 secretion⁵⁹. Within the hnRNPs group, hnRNPA3, hnRNPF and hnRNPD are all detected in
487 pathological inclusions of ALS and FTD brains^{56,60,61}. Moreover, hnRNPK is a regulator of
488 p53⁶², which we and others recently discovered was present in elevated amounts in AD
489 cortices^{11,12}. It has been also determined that hnRNPK sumoylation mediates p53 activity⁶³. All
490 this evidence places hnRNPs in a central position for further experimental analysis in human brain
491 tissues to elucidate more valuable information about the localization and function of this large
492 family of ribonucleoproteins.

493 HnRNPA3 has been identified in neuronal cytoplasmic and intranuclear inclusions in
494 patients with GGGGCC expansion repeats⁶¹ and hnRNP F were also found to co-localize with
495 GGGGCC expansion foci in immunoprecipitation studies⁶⁴. In addition, western blot analyses
496 imply that hnRNP may be in part responsible for the toxicity incurring by C9orf72 mutations,
497 considering important RNA processes such as splicing are compromised. hnRNP A3 and K have
498 been found associated with TDP-43⁶⁵. Implications of tau-mediated APAs in hnRNPs open new
499 venues for investigators to study new mechanistic insights of these proteins in several
500 proteinopathies. Within RBPs group, we also observed the *MATR3* gene. This gene encodes for
501 Matrin3, a DNA/RNA-binding protein. Mutations in this gene cause familial ALS/FTD, and *MATR3*
502 pathology is a feature of sporadic disease, suggesting that its dysfunction is inherently linked to
503 ALS pathogenesis⁶⁶.

504 Shorter 3'UTR are generally associated with enhanced translation of the mRNA APA in
505 the presence of WT tau, which supports the finding that high-levels of hnRNPs sustain dysfunction
506 of stress granules in ALS and FTD. Recent proteomic analysis in AD human Neurofibrillary
507 Tangles (NFTs) showed that phospho-tau in NFTs is associated with more than 500 proteins⁶⁷.
508 We observed several of these proteins in the APAs shortened WT tau, such as HNRNPK, ILF3,

509 AP2B1, RAN, RAB11A, HSP90B1, PARP1, MATR3, PPIA, NCL, HNRNPA3, HSP90AA1, and
510 HNRNPC. It is intriguing that the presence of chaperone Hsp90, a tau-regulated gene, plays a
511 crucial role in neurodegenerative pathologies and has been studied in AD or a long time⁶⁸.

512 These observations suggest that tau has early effects on gene expression that results in
513 later stages of toxic associations commonly found in neurodegeneration. Enrich-GO (Cellular
514 Function) of shortened-APAs genes by WT tau is provided in the supplemental information
515 section. GO-Cellular Process, Molecular Process and Cellular Components bar charts of
516 shortened APAs are shown in Fig S4.

517
518 **SWI/SFN, THO complexes, and several RNA-Binding protein precursors display**
519 **lengthened 3'UTRs in presence of WT tau.** Further analysis revealed 173 genes with
520 lengthened APAs. The complete list of the 173 genes with lengthened APAs is reported in the
521 supplemental information section. Among these genes, we found that many of them are related
522 to three major biological process: chromatin remodeling (GO:0006338), negative regulation of
523 gene expression (GO: 0010629), and mRNA processing (GO:0006397) (Fig 6A). To be more
524 specific, we noticed several genes belonging to the ATP-dependent chromatin remodeling
525 complex npBAF (mammalian SWI/SFN, GO: 0071564): *SMARCC2*, *ARID1A*, *SMARCA2* and
526 *SMARCA4*. This complex is found in neuronal progenitor's cells and post-mitotic neurons, and it
527 is essential for the maturation of the post-mitotic neuronal phenotype as well as long-term memory
528 formation⁶⁹. Along with the chromatin remodeling complex, other genes contained altered APAs,
529 including pericentric chromatin components (GO: 0005721, *HELLS* and *CBX3*), and nuclear
530 chromatin factors (GO:0000790, *SMARCC2*, *CBX3*, *H3F3A*, *NUCKS1*, *ARID1A*, *SMARCA2*,
531 *SMARCA4*, *HIST2H2AC*, *RAD50*, *NASP*, *MYC*, *NSMF*, *TCF3*) (Fig 6B).

532 Several nuclear speck (GO: 0016607) genes were also identified: *BASP1*, *POM*,; *ERBI*,
533 *YLPM1*, *HNRNPU*, *LUC7L3*, *CDC5L*, *TCF3*, *SRSF6*, and *KIF20B*. Cytoplasmic ribonucleoprotein

534 granule (GO: 0036464) and cytoplasmic stress granules (GO: 0010494) genes were delineated
535 as *MBNL1*, *CARHSP1*, *NCL*, *HNRNPU*, *IQGAP1*, *YBX1*, *RAC1*, *PABPC1*, *CNOT9*. Within the
536 domain of RNA processing, two genes *THOC2* and *THOC3* were also identified. They are
537 components of the THO complex (GO: 0000445) involved in efficient export of poly-adenylated
538 RNA and spliced RNAs²⁵.

539 The THO complex appears to coordinate transcripts for synapses development and
540 dopamine neuron survival⁷⁰. Recently, it has been found to interact with *ZC3H14*, which regulates
541 the processing of neuronal transcripts⁷¹, so it is not surprising to find in our dataset another
542 polyadenosine RNA-binding protein *ZC3H15* on the list of lengthened APAs. These observations
543 indicate that export complex RNA precursors are meaningfully affected by WT tau.

544 Not surprisingly, many translation initiation factors (GO: 0003743) were also discovered
545 in our analysis including *EIF2S3*, *EIF3E*, *EIF3A*, *EIF1*, and *EIF4G1*. It is important to note that
546 many APA-lengthened proteins in our study are RNA-Binding Proteins (RBPs). In fact, 46/173, or
547 ~27% of the total were. RBPs are implicated in the pathogenesis and progression of numerous
548 neurodegenerative diseases, and they are linked to toxic interactions and aggregations in
549 amyloidogenic proteins such Amyloid-beta and tau. The subsequent dysfunction of RBPs is
550 closely related to distinct pathways that are altered in proteinopathies⁷².

551 Considering the above, we also studied the presence of lengthened APAs of *ELAVL1*.
552 This gene encodes for HuR (RBPs), which is a neuroprotective protein. This protein has been
553 demonstrated in the regulation of oxidative metabolism in neurons as a way to protect from
554 neurodegeneration⁷³.

555 Apical dendrites (GO: 0097440) (*MAP1B*, *NSMF* and *CLU*) and other cytoskeletal genes
556 (*ACTR2*, *LIMA1*, *TPM4*, *PPP2R1A*, *BASP1*, *TARS*, *PHIP*, *NSMF*, *IQGAP1*, *RAC1*, *CLU*, and
557 *SMARCA2*) display lengthened poly-A tails as well. Enrich-GO (Cellular Function) of lengthened-

558 APAs genes in WT tau is provided in the supplemental information section. GO-Cellular Process,
559 Molecular Process and Cellular Components bar charts of lengthened-APAs are shown in Fig S4.
560

561 **P301L tau modulates 3'UTRs of RNA export complex THOC and splicing precursors**
562 **SNRPE**. In P301L tau precursor APAs, we detected 23 lengthened genes in total. More
563 specifically, the THOC2 gene, which is a component of the THO complex (GO: 0000445) was
564 lengthened in WT tau. Another gene of the small nuclear ribonucleoprotein complex (SNRPE)
565 was detected. *SNRPE* is also a gene for the spliceosome complex (GO: 0005681) (Fig 7A). Lastly,
566 the nuclear replication fork (GO: 0043596) gene *BAZ1B* was also observed.

567 In contrast to WT tau, P301L tau induces lengthening of the *HNRNPF* gene. HnRNPs
568 represent a large RNA-Binding protein family that contributes to many aspects of nucleic acid
569 metabolism, including alternative splicing, mRNA stabilization, transcriptional, and translational
570 regulation⁵⁵. Dysregulation of RNA metabolism is crucial in the pathogenesis of several
571 neurodegenerative diseases as Parkinson's⁷⁴, FTD and overlaps with aspects of ALS. Some
572 studies revealed possible involvement of hnRNPs in the pathogenesis and progression of these
573 diseases⁷⁵. Furthermore, hnRNP F has been uncovered in RNA foci in human brain tissue of FTD-
574 ALS patients⁵⁶. Affinity pull-down assays and genome-wide analysis also revealed a hnRNP F-
575 bound splicing complex that regulates neuronal and oligodendroglial differentiation pathways in
576 the developing brain⁶⁴. As observed for WT tau, the mutant P301L form also modulates several
577 RNA-Binding Proteins (GO: 0003723): *SLFN11*, *HNRNPF*, *FASN*, *HUWE1*, *PRRC2C*, *THOC2*,
578 *HMG2*, *SRSF7*, and *GIGYF7*. We found 34 genes in total with evidence of APA and shortened
579 3'UTRs (Fig 7B). The three top-scored cellular components were nuclear speck (GO: 0016607),
580 nuclear body (GO: 0016604) with *RBM39* (ALS associated gene⁷⁶) and Nuclear heterochromatin
581 genes (GO: 0005720). Nuclear speck and body genes consisted of *LUC7L3*, *SRSF4*, *NSRP1* and
582 *SRSF11*. Nuclear heterochromatin genes detected were *H2AFY* and *HIST1H1E*. *H2AFY* encodes

583 for a variant of the H2A histone that is present in a subset of nucleosomes where its role is to
584 represses transcription⁷⁷.

585 The Cellular Components scatterplot of lengthened APAs in WT Tau is presented in Fig
586 6C and GO Cellular component bar charts in Fig 6D.

587 These data suggest that the mutant P301L form of tau reduces activity in transcription and
588 alternative poly(A) tails processes due to loss-of-function. However, P301L tau does generate
589 different mRNA isoforms of transcripts mainly translated in splicing factors, nuclear speckle/body
590 structures and chromatin remodeling proteins. Enrich-GO (Cellular Function) of shortened and
591 lengthened-APAs by P301L tau is provided in the supplemental information section. GO-Cellular
592 Process, Molecular Process and Cellular Components bar charts of shortened and lengthened-
593 APAs are shown in Fig S4.

594

595

596

597

598

599

600

601

602

603

604

605

606

607

608 Discussion

609 In this study, we revealed new mechanistic insights into non-canonical tau functions. In particular,
610 we showed novel tau activities in transcription and alternative poly-adenylation (APA) pathways.
611 APA is a widespread mechanism of gene regulation that generates 3' ends in transcripts made
612 by RNA polymerase II⁷⁸. APA is regulated in cell proliferation, differentiation and extracellular
613 cues. It occurs in the 3'UTR and leads to the production of mRNA isoforms, followed by splicing
614 which leads to the production of distinct protein isoforms⁷⁸. Tau is typically described as an
615 abundant neuronal microtubule-binding protein. Recently, we observed its presence within non-
616 neuronal human cell lines and neuronal nuclei in AD brains ^{7,13} alongside other study². We were
617 particularly interested in the possibility of non-canonical tau functions. We hypothesized that
618 nuclear tau acts as a transcriptional regulator. To test our hypothesis, we used the tau inducible
619 HEK system, which is a well-established cell line capable of studying mechanisms related to the
620 tau aggregation process within a controlled system of MAPT gene expression⁷⁹. Our study
621 employed new technologies such as Poly(A)-ClickSeq to resolve whether genes were
622 upregulated or downregulated by WT and P301L tau in an *in-vitro* model. Furthermore, we
623 analyzed alternative polyadenylation (APA) profiles under the presence of WT and P301L tau⁷⁶.

624 Our results suggest that both WT and P301L tau are able to shuttle into the nuclei (Fig 4).
625 This observation confirmed our previous observations ⁷. We did not investigate the effect of the
626 P301L mutation on nuclei-cytoplasm shuttling in this report. The decreased number of genes
627 expressed in P301L cells suggests that this particular mutation of tau impairs transcriptional
628 activity. We did not investigate the LOF consequences of P301L tau in great detail, but our
629 observations suggest new mechanistic insights linked to alternative nuclear tau function.

630 One APA transcript of significance is the *SFPQ* gene, which we identified in WT tau
631 expression as having a lengthened 3'UTR. *SFPQ* has been associated with tau as a critical factor
632 for rapid progression of AD, and it has been observed as downregulated in post-mortem brain

633 tissue of rapidly progressive AD patients⁸⁰. Therefore, the lengthened APAs in this gene could
634 explain the down-regulation in the presence of a high level of tau, which mimics late-stage AD.
635 In-vitro data of SFPQ down-regulation due to human tau suggest a causal role of tau, possibly
636 through the alternative poly-adenylation of *SFPQ* transcripts.

637 Further analysis comparing 3'UTRs lengthened between WT and P301L tau revealed that
638 a significant number of RBPs showed lengthened 3'UTRs in P301L compared to WT tau. For
639 example, we detected 72 RBPs including *FUS* (found in the supplemental information section).
640 These data suggest a significant difference in RNA isoforms based on genetic tau background,
641 which then subsequently modulates different aspects of RNA metabolism in neurons.

642 Using the same cellular models, we determined that the prominent form of nuclear tau is
643 monomeric, but Tet induction causes tau oligomerization within the nuclei⁷. The formation of large
644 and nuclear oligomeric forms is another possible explanation for LOF observed as a consequence
645 of mutated tau. Mutant P301L tau shows a distinct aggregation mechanism compared to WT⁸¹
646 and aggregates faster than WT^{82,83}. For example, monomeric tau in the cytoplasm of cells
647 producing (WT or P301L) tau aggregate and subsequently avoid nuclear translocation. In
648 addition, aggregation in the cytoplasm and within the nuclei of tau reduces the pool of monomeric
649 nuclear tau. This pathological mechanism can compete with functional monomeric and oligomeric
650 tau, which then alters tau transcriptional activity. This phenomenon should be investigated in the
651 near future using neuronal models. Another function of tau is binding DNA in-vitro. Overall, the
652 multifunctional nature of nuclear tau should be thoroughly scrutinized in order to identify
653 unrevealed functions connected to DNA expression and RNA processing. We suggest that the
654 nature of nuclear tau as a transcriptional factor, chromatin remodeler and/or transcriptional co-
655 factor must be elucidated using proper models such as induced pluripotent stem cells or mouse
656 primary neurons carrying mutation on P301 site. At this stage, we can only hypothesize the direct
657 and indirect effects of tau during transcription.

658 This study utilized PAC-ClickSeq technology to identify the APA modulated by P301L and
659 WT tau. Alternative Poly-A (APA) sites in human genome have been identify mainly in 3'UTRs
660 (UTR-APA) sites, which harbor diverse regulatory sequences. This type of APA can change the
661 length and composition of 3'UTR, which subsequently affects the binding of miRNAs and/or
662 RBPs. This post-transcriptional modification leads to differences in mRNA stability, export,
663 localization, translational efficiency²⁶. Although the currently accepted theory is that genes with
664 longer 3'UTR tend to show decreased expression levels, this does not necessarily mean that
665 every single gene with a longer 3'UTR is less stable those with a shorter one.

666 We plan to investigate these findings using primary neurons and in-vivo models in the
667 near future. We are choosing these alternative models because the iHEK cell model have inherent
668 limitations in terms of reliability as a neuronal system. However, the iHEK cells used in this study
669 are an established model used by many researchers to study the mechanistic insights of tau
670 aggregation and toxicity. The results presented in this study support non-canonical functions of
671 tau. Therefore, we report broad tau-driven, post-transcriptional regulation in APAs by both WT
672 and P301L tau considering both cell lines produced high levels of monomeric and aggregated
673 tau. In this study, we did not investigate which tau isoform regulates APA in cells and by what
674 method tau regulates APAs, but we established a new category of interest in post-translational
675 modification. We hope further studies of nuclear tau and its relation to DNA and RNA processing
676 will identify new targets in tauopathies and eventually find new therapeutic targets.

677

678

679

680 **Limitations of the study.** As mentioned in the discussion, the main limitation of this study is the
681 nature of tau inducible HEK cells. We are aware that further study on neuronal cells is necessary.
682 However, iHEK models are commonly used to study mechanisms that are tau-dependent and
683 several of them have been translated into neurons models. All relevant datasets used and/or
684 analyzed in this current study are available upon request from the corresponding author.

685
686 **Supplemental Information.** The source data underlying all main and supplementary figures are
687 provided as a Source Data file. RNAseq datasets is uploaded to NCBI SRA, reference number:
688 [PRJNA744518](#). Figure 1A, 4F and 7C were generated using BioRender Software
689 (<https://biorender.com>).

690
691 **Acknowledgments and Funding.** We thank the members of the Kayed and Routh labs for their
692 support and help. We thank Bergman Isabelle B. and Leiana Fung for editing and proofreading
693 of the manuscript. This work was supported by Mitchell Center for Neurodegenerative Diseases,
694 the Gillson Longenbaugh Foundation and National Institute of Health grants: R01AG054025,
695 R01NS094557, R01AG055771, R01AG060718 and the American Heart Association collaborative
696 grant 17CSA33620007 (R.K.).

697
698 **Author contribution.** Conceptualization, M.M., A.R. and R.K.; Methodology, M.M., A.R. and
699 R.K.; Investigation, M.M., E.J., S.M., A.E. and S.G.; Transcriptomic analysis, A.R. and E.J.;
700 Writing – Original Draft, M.M.; Writing – Review & Editing, all authors; Funding Acquisition, R.K.;
701 Resources, R.K.; Supervision, M.M. and R.K.

702
703 **Declaration of Interests**
704 The authors declare no competing interests.

705

706 **References**

707

- 708 1. Sultan A, Nessler F, Violet M, et al. Nuclear tau, a key player in neuronal DNA
709 protection. *The Journal of biological chemistry*. 2011;286(6):4566-4575.
710 doi:10.1074/jbc.M110.199976
- 711 2. Violet M, Delattre L, Tardivel M, et al. A major role for Tau in neuronal DNA and RNA
712 protection in vivo under physiological and hyperthermic conditions. *Frontiers in cellular*
713 *neuroscience*. 2014;8:84. doi:10.3389/fncel.2014.00084
- 714 3. Hua Q, He R. Tau could protect DNA double helix structure. *Biochimica et biophysica*
715 *acta*. 2003;1645(2):205-211. doi:10.1016/s1570-9639(02)00538-1
- 716 4. Zhang X, Lin Y, Eschmann NA, et al. RNA stores tau reversibly in complex coacervates.
717 *PLoS biology*. 2017;15(7):e2002183. doi:10.1371/journal.pbio.2002183
- 718 5. Kampers T, Friedhoff P, Biernat J, Mandelkow EM, Mandelkow E. RNA stimulates
719 aggregation of microtubule-associated protein tau into Alzheimer-like paired helical
720 filaments. *FEBS letters*. 1996;399(3):344-349. doi:10.1016/s0014-5793(96)01386-5
- 721 6. Monroy-Ramírez HC, Basurto-Islas G, Mena R, et al. Alterations in the nuclear
722 architecture produced by the overexpression of tau protein in neuroblastoma cells.
723 *Journal of Alzheimer's disease : JAD*. 2013;36(3):503-520. doi:10.3233/JAD-122401
- 724 7. Montalbano M, McAllen S, Sengupta U, et al. Tau oligomers mediate aggregation of RNA-
725 binding proteins Musashi1 and Musashi2 inducing Lamin alteration. *Aging cell*. Published
726 online September 2019:e13035. doi:10.1111/accel.13035
- 727 8. Loomis PA, Howard TH, Castleberry RP, Binder LI. Identification of nuclear tau isoforms in
728 human neuroblastoma cells. *Proceedings of the National Academy of Sciences of the*
729 *United States of America*. 1990;87(21):8422-8426. doi:10.1073/pnas.87.21.8422
- 730 9. Shea TB, Cressman CM. A 26-30 kDa developmentally-regulated tau isoform localized
731 within nuclei of mitotic human neuroblastoma cells. *International journal of*
732 *developmental neuroscience : the official journal of the International Society for*
733 *Developmental Neuroscience*. 1998;16(1):41-48. doi:10.1016/s0736-5748(97)00044-0
- 734 10. Ulrich G, Salvade A, Boersema P, et al. Phosphorylation of nuclear Tau is modulated by
735 distinct cellular pathways. *Scientific reports*. 2018;8(1):17702. doi:10.1038/s41598-018-
736 36374-4
- 737 11. Baquero J, Varriano S, Ordonez M, et al. Nuclear Tau, p53 and Pin1 Regulate PARN-
738 Mediated Deadenylation and Gene Expression. *Frontiers in Molecular Neuroscience*.
739 2019;12:242. doi:10.3389/fnmol.2019.00242
- 740 12. Farmer KM, Ghag G, Puangmalai N, Montalbano M, Bhatt N, Kaye R. P53 aggregation,
741 interactions with tau, and impaired DNA damage response in Alzheimer's disease. *Acta*
742 *Neuropathologica Communications*. 2020;8(1):132. doi:10.1186/s40478-020-01012-6
- 743 13. Montalbano M, McAllen S, Puangmalai N, et al. RNA-binding proteins Musashi and tau
744 soluble aggregates initiate nuclear dysfunction. *Nature Communications*.
745 2020;11(1):4305. doi:10.1038/s41467-020-18022-6
- 746 14. Venkatramani A, Panda D. Regulation of neuronal microtubule dynamics by tau:
747 Implications for tauopathies. *International journal of biological macromolecules*.
748 2019;133:473-483. doi:10.1016/j.ijbiomac.2019.04.120

- 749 15. Maina MB, Bailey LJ, Wagih S, et al. The involvement of tau in nucleolar transcription and
750 the stress response. *Acta neuropathologica communications*. 2018;6(1):70.
751 doi:10.1186/s40478-018-0565-6
- 752 16. Maina MB, Bailey LJ, Doherty AJ, Serpell LC. The Involvement of Abeta42 and Tau in
753 Nucleolar and Protein Synthesis Machinery Dysfunction. *Frontiers in cellular*
754 *neuroscience*. 2018;12:220. doi:10.3389/fncel.2018.00220
- 755 17. Lester E, Parker R. The Tau of Nuclear-Cytoplasmic Transport. *Neuron*. 2018;99(5):869-
756 871. doi:10.1016/j.neuron.2018.08.026
- 757 18. Paonessa F, Evans LD, Solanki R, et al. Microtubules Deform the Nuclear Membrane and
758 Disrupt Nucleocytoplasmic Transport in Tau-Mediated Frontotemporal Dementia. *Cell*
759 *reports*. 2019;26(3):582-593.e5. doi:10.1016/j.celrep.2018.12.085
- 760 19. Tripathi T, Prakash J, Shav-Tal Y. Phospho-Tau Impairs Nuclear-Cytoplasmic Transport.
761 *ACS chemical neuroscience*. 2019;10(1):36-38. doi:10.1021/acscchemneuro.8b00632
- 762 20. Eftekharzadeh B, Daigle JG, Kapinos LE, et al. Tau Protein Disrupts Nucleocytoplasmic
763 Transport in Alzheimer's Disease. *Neuron*. 2018;99(5):925-940.e7.
764 doi:10.1016/j.neuron.2018.07.039
- 765 21. Siano G, Varisco M, Caiazza MC, et al. Tau Modulates VGLUT1 Expression. *Journal of*
766 *molecular biology*. 2019;431(4):873-884. doi:10.1016/j.jmb.2019.01.023
- 767 22. Klein H-U, McCabe C, Gjoneska E, et al. Epigenome-wide study uncovers large-scale
768 changes in histone acetylation driven by tau pathology in aging and Alzheimer's human
769 brains. *Nature neuroscience*. 2019;22(1):37-46. doi:10.1038/s41593-018-0291-1
- 770 23. Mansuroglu Z, Benhelli-Mokrani H, Marcato V, et al. Loss of Tau protein affects the
771 structure, transcription and repair of neuronal pericentromeric heterochromatin.
772 *Scientific reports*. 2016;6:33047. doi:10.1038/srep33047
- 773 24. Benhelli-Mokrani H, Mansuroglu Z, Chauderlier A, et al. Genome-wide identification of
774 genic and intergenic neuronal DNA regions bound by Tau protein under physiological
775 and stress conditions. *Nucleic acids research*. 2018;46(21):11405-11422.
776 doi:10.1093/nar/gky929
- 777 25. Stewart M. Polyadenylation and nuclear export of mRNAs. *The Journal of biological*
778 *chemistry*. 2019;294(9):2977-2987. doi:10.1074/jbc.REV118.005594
- 779 26. Gruber AJ, Zavolan M. Alternative cleavage and polyadenylation in health and disease.
780 *Nature Reviews Genetics*. 2019;20(10):599-614. doi:10.1038/s41576-019-0145-z
- 781 27. Tian B, Hu J, Zhang H, Lutz CS. A large-scale analysis of mRNA polyadenylation of human
782 and mouse genes. *Nucleic Acids Research*. 2005;33(1):201-212. doi:10.1093/nar/gki158
- 783 28. Shepard PJ, Choi E-A, Lu J, Flanagan LA, Hertel KJ, Shi Y. Complex and dynamic landscape
784 of RNA polyadenylation revealed by PAS-Seq. *RNA (New York, NY)*. 2011;17(4):761-772.
785 doi:10.1261/rna.2581711
- 786 29. Rio DC, Ares MJ, Hannon GJ, Nilsen TW. Purification of RNA using TRIzol (TRI reagent).
787 *Cold Spring Harbor protocols*. 2010;2010(6):pdb.prot5439. doi:10.1101/pdb.prot5439
- 788 30. Jaworski E, Routh A. ClickSeq: Replacing Fragmentation and Enzymatic Ligation with
789 Click-Chemistry to Prevent Sequence Chimeras. *Methods in molecular biology (Clifton,*
790 *NJ)*. 2018;1712:71-85. doi:10.1007/978-1-4939-7514-3_6
- 791 31. Elrod ND, Jaworski EA, Ji P, Wagner EJ, Routh A. Development of Poly(A)-ClickSeq as a
792 tool enabling simultaneous genome-wide poly(A)-site identification and differential

- 793 expression analysis. *Methods (San Diego, Calif)*. 2019;155:20-29.
794 doi:10.1016/j.ymeth.2019.01.002
- 795 32. Routh A. DPAC: A Tool for Differential Poly(A)-Cluster Usage from Poly(A)-Targeted
796 RNAseq Data. *G3 (Bethesda, Md)*. 2019;9(6):1825-1830. doi:10.1534/g3.119.400273
- 797 33. Kim D, Paggi JM, Park C, Bennett C, Salzberg SL. Graph-based genome alignment and
798 genotyping with HISAT2 and HISAT-genotype. *Nature Biotechnology*. 2019;37(8):907-915.
799 doi:10.1038/s41587-019-0201-4
- 800 34. Kuleshov M v, Jones MR, Rouillard AD, et al. Enrichr: a comprehensive gene set
801 enrichment analysis web server 2016 update. *Nucleic Acids Research*. 2016;44(W1):W90-
802 W97. doi:10.1093/nar/gkw377
- 803 35. Miyasaka T, Shinzaki Y, Yoshimura S, et al. Imbalanced Expression of Tau and Tubulin
804 Induces Neuronal Dysfunction in *C. elegans* Models of Tauopathy. *Frontiers in*
805 *Neuroscience*. 2018;12:415. doi:10.3389/fnins.2018.00415
- 806 36. Bittermann E, Abdelhamed Z, Liegel RP, et al. Differential requirements of tubulin genes
807 in mammalian forebrain development. *PLOS Genetics*. 2019;15(8):e1008243.
808 <https://doi.org/10.1371/journal.pgen.1008243>
- 809 37. Kwon HS, Koh S-H. Neuroinflammation in neurodegenerative disorders: the roles of
810 microglia and astrocytes. *Translational Neurodegeneration*. 2020;9(1):42.
811 doi:10.1186/s40035-020-00221-2
- 812 38. Morales I, Jiménez JM, Mancilla M, Maccioni RB. Tau oligomers and fibrils induce
813 activation of microglial cells. *Journal of Alzheimer's disease : JAD*. 2013;37(4):849-856.
814 doi:10.3233/JAD-131843
- 815 39. Karch CM, Goate AM. Alzheimer's disease risk genes and mechanisms of disease
816 pathogenesis. *Biological psychiatry*. 2015;77(1):43-51.
817 doi:10.1016/j.biopsych.2014.05.006
- 818 40. Niday Z, Hawkins VE, Soh H, Mulkey DK, Tzingounis A v. Epilepsy-Associated KCNQ2
819 Channels Regulate Multiple Intrinsic Properties of Layer 2/3 Pyramidal Neurons. *The*
820 *Journal of neuroscience : the official journal of the Society for Neuroscience*.
821 2017;37(3):576-586. doi:10.1523/JNEUROSCI.1425-16.2016
- 822 41. Short B, Preisinger C, Körner R, Kopajtich R, Byron O, Barr FA. A GRASP55-rab2 effector
823 complex linking Golgi structure to membrane traffic. *Journal of Cell Biology*.
824 2001;155(6):877-884. doi:10.1083/jcb.200108079
- 825 42. Ito D, Walker JR, Thompson CS, et al. Characterization of stanniocalcin 2, a novel target
826 of the mammalian unfolded protein response with cytoprotective properties. *Molecular*
827 *and cellular biology*. 2004;24(21):9456-9469. doi:10.1128/MCB.24.21.9456-9469.2004
- 828 43. Bemben MA, Shipman SL, Nicoll RA, Roche KW. The cellular and molecular landscape of
829 neuroligins. *Trends in neurosciences*. 2015;38(8):496-505. doi:10.1016/j.tins.2015.06.004
- 830 44. Brito-Moreira J, Lourenco M v, Oliveira MM, et al. Interaction of amyloid- β (A β)
831 oligomers with neurexin 2 α and neuroligin 1 mediates synapse damage and memory loss
832 in mice. *The Journal of biological chemistry*. 2017;292(18):7327-7337.
833 doi:10.1074/jbc.M116.761189
- 834 45. Dufort-Gervais J, Provost C, Charbonneau L, et al. Neuroligin-1 is altered in the
835 hippocampus of Alzheimer's disease patients and mouse models, and modulates the

- 836 toxicity of amyloid-beta oligomers. *Scientific reports*. 2020;10(1):6956.
837 doi:10.1038/s41598-020-63255-6
- 838 46. Craig AM, Kang Y. Neurexin-neurologin signaling in synapse development. *Current opinion*
839 *in neurobiology*. 2007;17(1):43-52. doi:10.1016/j.conb.2007.01.011
- 840 47. Helou J el, Bélanger-Nelson E, Freyburger M, et al. Neurologin-1 links neuronal activity to
841 sleep-wake regulation. *Proceedings of the National Academy of Sciences of the United*
842 *States of America*. 2013;110(24):9974-9979. <http://www.jstor.org/stable/42706115>
- 843 48. Wu X, Morishita WK, Riley AM, Hale WD, Südhof TC, Malenka RC. Neurologin-1 Signaling
844 Controls LTP and NMDA Receptors by Distinct Molecular Pathways. *Neuron*.
845 2019;102(3):621-635.e3. doi:10.1016/j.neuron.2019.02.013
- 846 49. Lee S-H, Peng I-F, Ng YG, et al. Synapses are regulated by the cytoplasmic tyrosine kinase
847 Fer in a pathway mediated by p120catenin, Fer, SHP-2, and beta-catenin. *The Journal of*
848 *cell biology*. 2008;183(5):893-908. doi:10.1083/jcb.200807188
- 849 50. Patrón LA, Nagatomo K, Eves DT, et al. Cul4 ubiquitin ligase cofactor DCAF12 promotes
850 neurotransmitter release and homeostatic plasticity. *The Journal of cell biology*.
851 2019;218(3):993-1010. doi:10.1083/jcb.201805099
- 852 51. Zheng C, Geetha T, Babu JR. Failure of ubiquitin proteasome system: risk for
853 neurodegenerative diseases. *Neuro-degenerative diseases*. 2014;14(4):161-175.
854 doi:10.1159/000367694
- 855 52. Paudel YN, Angelopoulou E, Piperi C, Othman I, Aamir K, Shaikh MF. Impact of HMGB1,
856 RAGE, and TLR4 in Alzheimer's Disease (AD): From Risk Factors to Therapeutic Targeting.
857 *Cells*. 2020;9(2). doi:10.3390/cells9020383
- 858 53. Yatskevich S, Rhodes J, Nasmyth K. Organization of Chromosomal DNA by SMC
859 Complexes. *Annual review of genetics*. 2019;53:445-482. doi:10.1146/annurev-genet-
860 112618-043633
- 861 54. Aragon L, Martinez-Perez E, Merkschlager M. Condensin, cohesin and the control of
862 chromatin states. *Current opinion in genetics & development*. 2013;23(2):204-211.
863 doi:10.1016/j.gde.2012.11.004
- 864 55. Geuens T, Bouhy D, Timmerman V. The hnRNP family: insights into their role in health
865 and disease. *Human genetics*. 2016;135(8):851-867. doi:10.1007/s00439-016-1683-5
- 866 56. Lee Y-B, Chen H-J, Peres JN, et al. Hexanucleotide Repeats in ALS/FTD Form Length-
867 Dependent RNA Foci, Sequester RNA Binding Proteins, and Are Neurotoxic. *Cell Reports*.
868 2013;5(5):1178-1186. doi:<https://doi.org/10.1016/j.celrep.2013.10.049>
- 869 57. Liu Y, Szaro BG. hnRNP K post-transcriptionally co-regulates multiple cytoskeletal genes
870 needed for axonogenesis. *Development*. 2011;138(14):3079 LP - 3090.
871 doi:10.1242/dev.066993
- 872 58. Lee EK, Kim HH, Kuwano Y, et al. hnRNP C promotes APP translation by competing with
873 FMRP for APP mRNA recruitment to P bodies. *Nature structural & molecular biology*.
874 2010;17(6):732-739. doi:10.1038/nsmb.1815
- 875 59. Rajagopalan LE, Westmark CJ, Jarzembowski JA, Malter JS. hnRNP C increases amyloid
876 precursor protein (APP) production by stabilizing APP mRNA. *Nucleic acids research*.
877 1998;26(14):3418-3423. doi:10.1093/nar/26.14.3418
- 878 60. Gami-Patel P, Bandopadhyay R, Brelstaff J, Revesz T, Lashley T. The presence of
879 heterogeneous nuclear ribonucleoproteins in frontotemporal lobar degeneration with

- 880 FUS-positive inclusions. *Neurobiology of aging*. 2016;46:192-203.
881 doi:10.1016/j.neurobiolaging.2016.07.004
- 882 61. Mori K, Lammich S, Mackenzie IRA, et al. hnRNP A3 binds to GGGGCC repeats and is a
883 constituent of p62-positive/TDP43-negative inclusions in the hippocampus of patients
884 with C9orf72 mutations. *Acta neuropathologica*. 2013;125(3):413-423.
885 doi:10.1007/s00401-013-1088-7
- 886 62. Low Y-H, Asi Y, Foti SC, Lashley T. Heterogeneous Nuclear Ribonucleoproteins:
887 Implications in Neurological Diseases. *Molecular Neurobiology*. 2021;58(2):631-646.
888 doi:10.1007/s12035-020-02137-4
- 889 63. Pelisch F, Pozzi B, Risso G, Muñoz MJ, Srebrow A. DNA damage-induced heterogeneous
890 nuclear ribonucleoprotein K sumoylation regulates p53 transcriptional activation. *The*
891 *Journal of biological chemistry*. 2012;287(36):30789-30799.
892 doi:10.1074/jbc.M112.390120
- 893 64. Mandler MD, Ku L, Feng Y. A cytoplasmic quaking I isoform regulates the hnRNP F/H-
894 dependent alternative splicing pathway in myelinating glia. *Nucleic Acids Research*.
895 2014;42(11):7319-7329. doi:10.1093/nar/gku353
- 896 65. Moujalled D, Grubman A, Acevedo K, et al. TDP-43 mutations causing amyotrophic lateral
897 sclerosis are associated with altered expression of RNA-binding protein hnRNP K and
898 affect the Nrf2 antioxidant pathway. *Human Molecular Genetics*. 2017;26(9):1732-1746.
899 doi:10.1093/hmg/ddx093
- 900 66. Malik AM, Miguez RA, Li X, Ho Y-S, Feldman EL, Barmada SJ. Matrin 3-dependent
901 neurotoxicity is modified by nucleic acid binding and nucleocytoplasmic localization.
902 Taylor JP, ed. *eLife*. 2018;7:e35977. doi:10.7554/eLife.35977
- 903 67. Drummond E, Pires G, MacMurray C, et al. Phosphorylated tau interactome in the human
904 Alzheimer's disease brain. *Brain : a journal of neurology*. 2020;143(9):2803-2817.
905 doi:10.1093/brain/awaa223
- 906 68. Campanella C, Pace A, Caruso Bavisotto C, et al. Heat Shock Proteins in Alzheimer's
907 Disease: Role and Targeting. *International Journal of Molecular Sciences* . 2018;19(9).
908 doi:10.3390/ijms19092603
- 909 69. Sokpor G, Xie Y, Rosenbusch J, Tuoc T. Chromatin Remodeling BAF (SWI/SNF) Complexes
910 in Neural Development and Disorders. *Frontiers in molecular neuroscience*. 2017;10:243.
911 doi:10.3389/fnmol.2017.00243
- 912 70. Maeder CI, Kim J-I, Liang X, et al. The THO Complex Coordinates Transcripts for Synapse
913 Development and Dopamine Neuron Survival. *Cell*. 2018;174(6):1436-1449.e20.
914 doi:10.1016/j.cell.2018.07.046
- 915 71. Morris KJ, Corbett AH. The polyadenosine RNA-binding protein ZC3H14 interacts with the
916 THO complex and coordinately regulates the processing of neuronal transcripts. *Nucleic*
917 *acids research*. 2018;46(13):6561-6575. doi:10.1093/nar/gky446
- 918 72. Maziuk B, Ballance HI, Wolozin B. Dysregulation of RNA Binding Protein Aggregation in
919 Neurodegenerative Disorders. *Frontiers in molecular neuroscience*. 2017;10:89.
920 doi:10.3389/fnmol.2017.00089
- 921 73. Skliris A, Papadaki O, Kafasla P, et al. Neuroprotection requires the functions of the RNA-
922 binding protein HuR. *Cell death and differentiation*. 2015;22(5):703-718.
923 doi:10.1038/cdd.2014.158

- 924 74. Lu B, Gehrke S, Wu Z. RNA metabolism in the pathogenesis of Parkinson's disease. *Brain*
925 *research*. 2014;1584:105-115. doi:10.1016/j.brainres.2014.03.003
- 926 75. Bampton A, Gittings LM, Fratta P, Lashley T, Gatt A. The role of hnRNPs in frontotemporal
927 dementia and amyotrophic lateral sclerosis. *Acta Neuropathologica*. 2020;140(5):599-
928 623. doi:10.1007/s00401-020-02203-0
- 929 76. Couthouis J, Hart MP, Shorter J, et al. A yeast functional screen predicts new candidate
930 ALS disease genes. *Proceedings of the National Academy of Sciences of the United States*
931 *of America*. 2011;108(52):20881-20890. doi:10.1073/pnas.1109434108
- 932 77. Doyen C-M, An W, Angelov D, et al. Mechanism of polymerase II transcription repression
933 by the histone variant macroH2A. *Molecular and cellular biology*. 2006;26(3):1156-1164.
934 doi:10.1128/MCB.26.3.1156-1164.2006
- 935 78. Tian B, Manley JL. Alternative cleavage and polyadenylation: the long and short of it.
936 *Trends in biochemical sciences*. 2013;38(6):312-320. doi:10.1016/j.tibs.2013.03.005
- 937 79. Koren SA, Hamm MJ, Meier SE, et al. Tau drives translational selectivity by interacting
938 with ribosomal proteins. *Acta Neuropathologica*. 2019;137(4):571-583.
939 doi:10.1007/s00401-019-01970-9
- 940 80. Younas N, Zafar S, Shafiq M, et al. SFPQ and Tau: critical factors contributing to rapid
941 progression of Alzheimer's disease. *Acta neuropathologica*. 2020;140(3):317-339.
942 doi:10.1007/s00401-020-02178-y
- 943 81. Strang KH, Croft CL, Sorrentino ZA, Chakrabarty P, Golde TE, Giasson BI. Distinct
944 differences in prion-like seeding and aggregation between Tau protein variants provide
945 mechanistic insights into tauopathies. *The Journal of biological chemistry*.
946 2018;293(7):2408-2421. doi:10.1074/jbc.M117.815357
- 947 82. Aoyagi H, Hasegawa M, Tamaoka A. Fibrillogenic nuclei composed of P301L mutant tau
948 induce elongation of P301L tau but not wild-type tau. *The Journal of biological*
949 *chemistry*. 2007;282(28):20309-20318. doi:10.1074/jbc.M611876200
- 950 83. Barghorn S, Zheng-Fischhöfer Q, Ackmann M, et al. Structure, microtubule interactions,
951 and paired helical filament aggregation by tau mutants of frontotemporal dementias.
952 *Biochemistry*. 2000;39(38):11714-11721. doi:10.1021/bi000850r
953
954

955 Figure Legends

956

957 **Fig 1. Tau-dependent Gene expression.** (A) Schematic representation of experimental plan, from Tet
958 induction in WT and P301L Tau iHEK to RNA isolation, sequencing to gene expression analysis. (B)
959 Volcano Plot for Down- and Up-regulated gene in WT Tau iHEK. (C) Volcano Plot for Down- and Up-
960 regulated gene in P301L Tau iHEK. (D) Gene Lists of Down-Regulated (Red Boxes) and Up-Regulated
961 (Green Boxes) Genes in WT Tau iHEK. (E) Gene Lists of Down-Regulated (Red Boxes) and Up-Regulated
962 (Green Boxes) Genes in P301L Tau iHEK.

963

964 **Fig 2. Up- and Down regulated genes in WT Tau iHEK Gene Ontology.** Left Column (Green) Up-
965 regulated genes analyzed by Enrich GO and divided by Biological Process, Molecular Function and Cellular
966 Component. Right Column (Blue) Down-regulated genes analyzed by Enrich GO and divided by Biological
967 Process, Molecular Function and Cellular Component. Grey bars represent not significant correlation.

968

969 **Fig 3. WT tau modulates gene expression of chromatin organization and remodeling factors.** (A)
970 Enrichment plot for GO Chromatin organization. (B) Enrichment plot for GO Chromatin remodeling. (C)
971 Enrichment plot for GO-Covalent Chromatin modification. (D) IB of Up-regulated genes: RCC1, DNAJC2
972 and Histone 1.2 (red box) and Down-regulated genes: SMARCC1, SMARCA5 and HMGB1 (blue box) in
973 cytoplasm and nuclear fractions from WT and P301L Tau iHEK. Histone 3 and β -Actin has been used as
974 loading control for nuclear and cytoplasmic fractions, respectively. (E) representative Tau 13 (magenta)
975 and Histone 1.2 (green) Co-IF of control (-Tet) and treated WT Tau iHEK. (F) Histone 1.2 integrated density
976 quantification in control and +Tet cells (Unpaired t-test, $p < 0.0001$, ****). (G) representative Tau 13
977 (magenta) and Ki67 (green) Co-IF of control (-Tet) and treated WT Tau iHEK. (H) Ki67 integrated density
978 quantification in control and +Tet cells (Unpaired t-test, $p < 0.0001$, ****). (I) representative Tau 13 (magenta)
979 and SMARCC1 (green) Co-IF of control (-Tet) and treated WT Tau iHEK. (J) SMARCC1 integrated density
980 quantification in control and +Tet cells (Unpaired t-test, $p < 0.0001$, ****). (K) representative Tau 13 (magenta)
981 and SMARCA5 (green) Co-IF of control (-Tet) and treated WT Tau iHEK. (L) SMARCA5 integrated density
982 quantification in control and +Tet cells (Unpaired t-test, $p < 0.0001$, ****).

983

984 **Fig 4. Tau nuclear shuttling.** (A) GWAS GO-Histone Binding heat map in WT Tau. (B) GWAS GO-
985 Nucleosome organization heat map in WT Tau. (C) Enrichment plot for GO Histone Binding. (D) Enrichment
986 plot for GO Nucleosome Organization. (E) Immunoblot (IB) with Tau13 (1:1000) and β -Actin () of cytoplasm
987 and nuclear fraction from WT (left panel) and P301L (right panel) Tau induced with Tet. (F) Relative density
988 of nuclear monomeric Tau ($m\tau_{N}$, normalized with Histone3). Unpaired *t*-test has been performed to
989 compare column means ((-) WT Tau vs WT Tau ***, $p = 0.0009$, (-) p301l Tau vs P301L Tau *, $p = 0.0169$,
990 WT Tau vs P301L Tau **, $p = 0.0065$). (G) Schematic model on Tau nuclear import in the two iHEK cell lines.

991

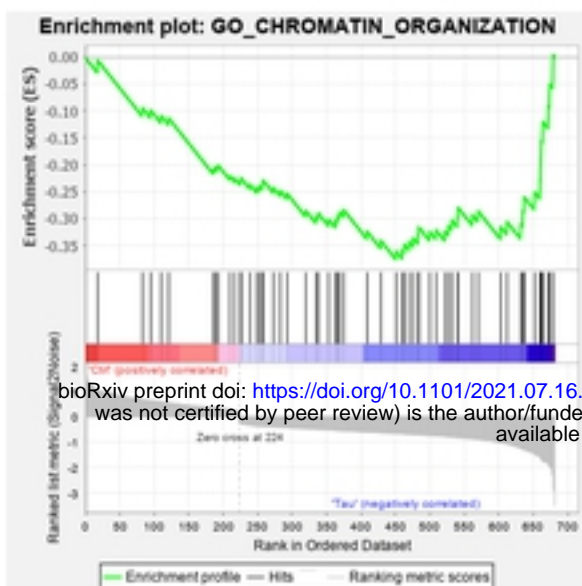
992 **Fig 5. RNA metabolism, chromatin organization and HNRNPs precursor's display shortened APAs**
993 **in the presence of WT tau.** (A) Enrich-GO Biological Process of WT Tau shortened APAs (p -value
994 reported). (B) Partial list of biological process genes with shortened APAs upon presence of WT Tau
995 (mRNA processing, RNA splicing, chromatin remodeling and regulation of response to DNA damage). (C)
996 The Cellular Components scatterplot is organized so that similar gene sets are clustered together. The
997 larger blue points represent significantly enriched terms - the darker the blue, the more significant the term
998 and the smaller the p -value. The gray points are not significant. Plots has been generated and downloaded
999 using scatter plot visualization Appyter. (D) Enrich-GO Cellular Component of WT Tau shortened APAs (p -
1000 value reported).

1001

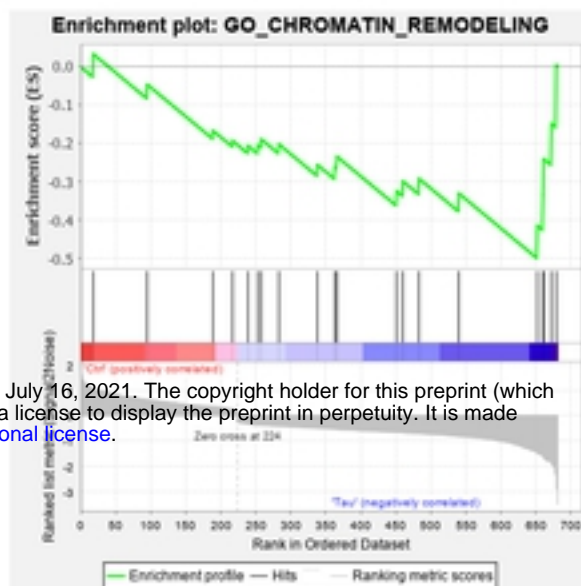
1002 **Fig 6. RNA processing and splicing precursor's display lengthened APAs in presence of WT tau.**
1003 (A) Enrich-GO Biological Process of WT Tau lengthened APAs (p-value reported). (B) Partial list of
1004 biological process genes with lengthened APAs upon presence of WT Tau negative control of gene
1005 expression, chromatin remodeling, nucleosome organization, mRNA processing and regulation of
1006 transcription). (C) The Cellular Components scatterplot of lengthened APAs in WT Tau is organized so that
1007 similar gene sets are clustered together. The larger blue points represent significantly enriched terms - the
1008 darker the blue, the more significant the term and the smaller the p-value. The gray points are not significant.
1009 Plots has been generated and downloaded using scatter plot visualization Appyter. (d) Enrich-GO Cellular
1010 Component of WT Tau lengthened APAs (p-value reported).

1011
1012 **Fig 7. Mutant P301L Tau modulates APAs associated with spliceosome and nuclear chromatin. (A)**
1013 Scatterplot of gene clusters from lengthened mRNA precursors upon P301L Tau expression. (B) Scatterplot
1014 of gene clusters from shortened mRNA precursors upon P301L Tau expression. (C) Model for nuclear Tau
1015 activity to transcriptional and post-transcriptional levels.
1016

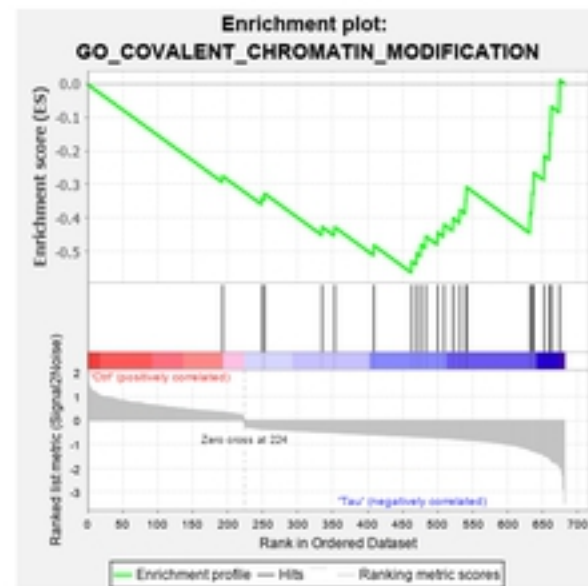
A



B

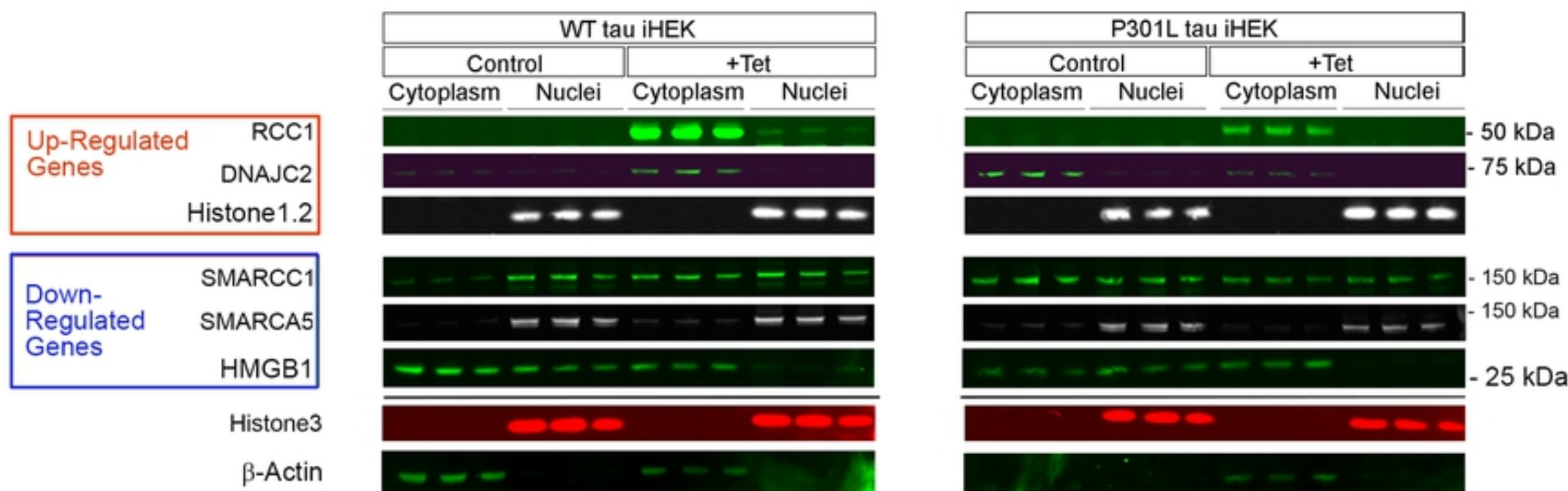


C

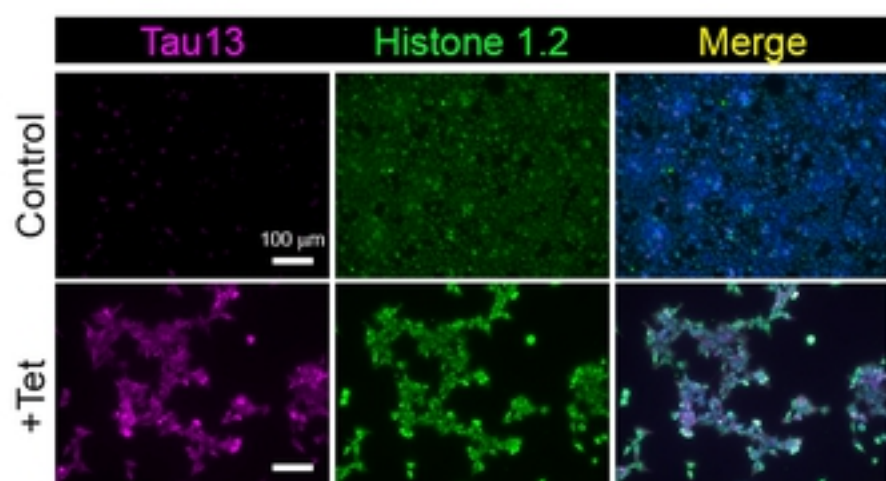


bioRxiv preprint doi: <https://doi.org/10.1101/2021.07.16.452616>; this version posted July 16, 2021. The copyright holder for this preprint (which was not certified by peer review) is the author/funder, who has granted bioRxiv a license to display the preprint in perpetuity. It is made available under aCC-BY 4.0 International license.

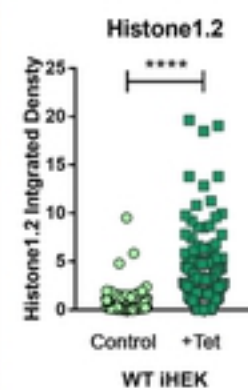
D



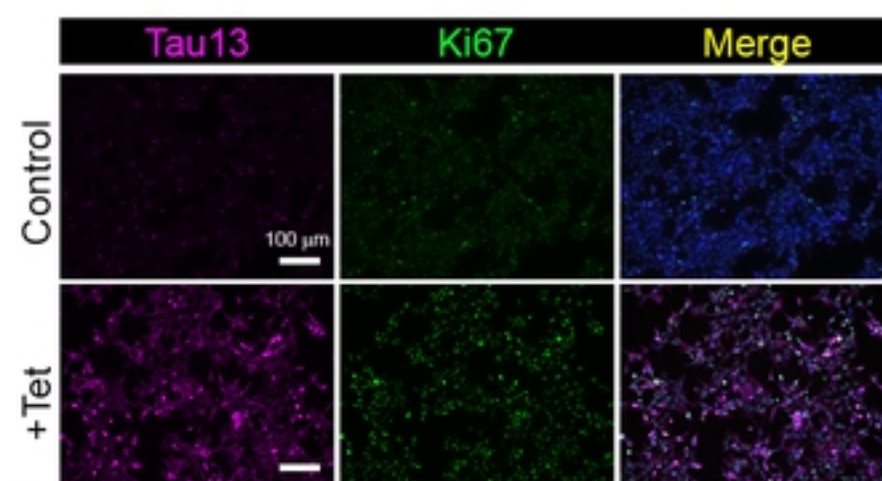
E



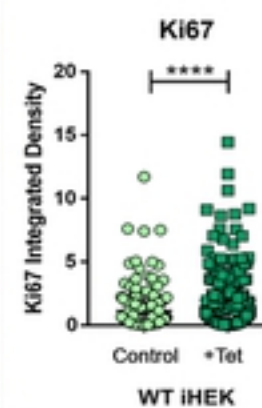
F



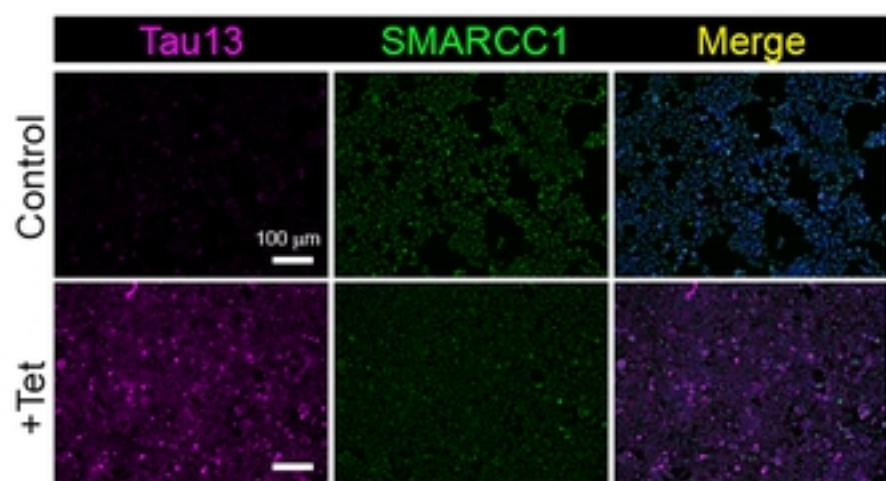
G



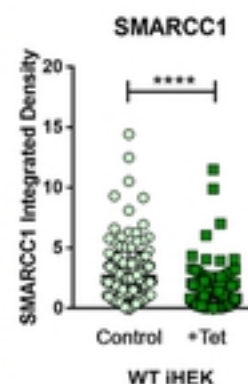
H



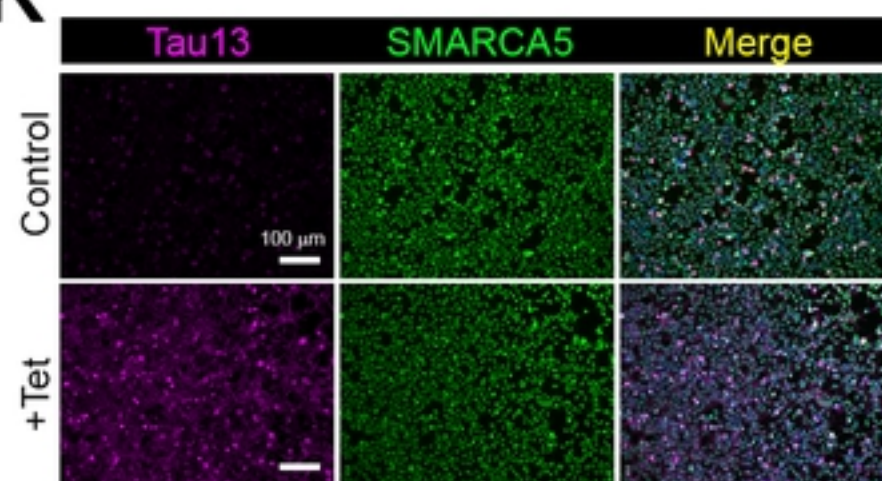
I



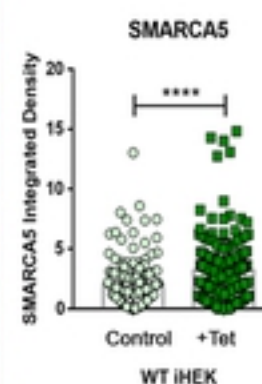
J

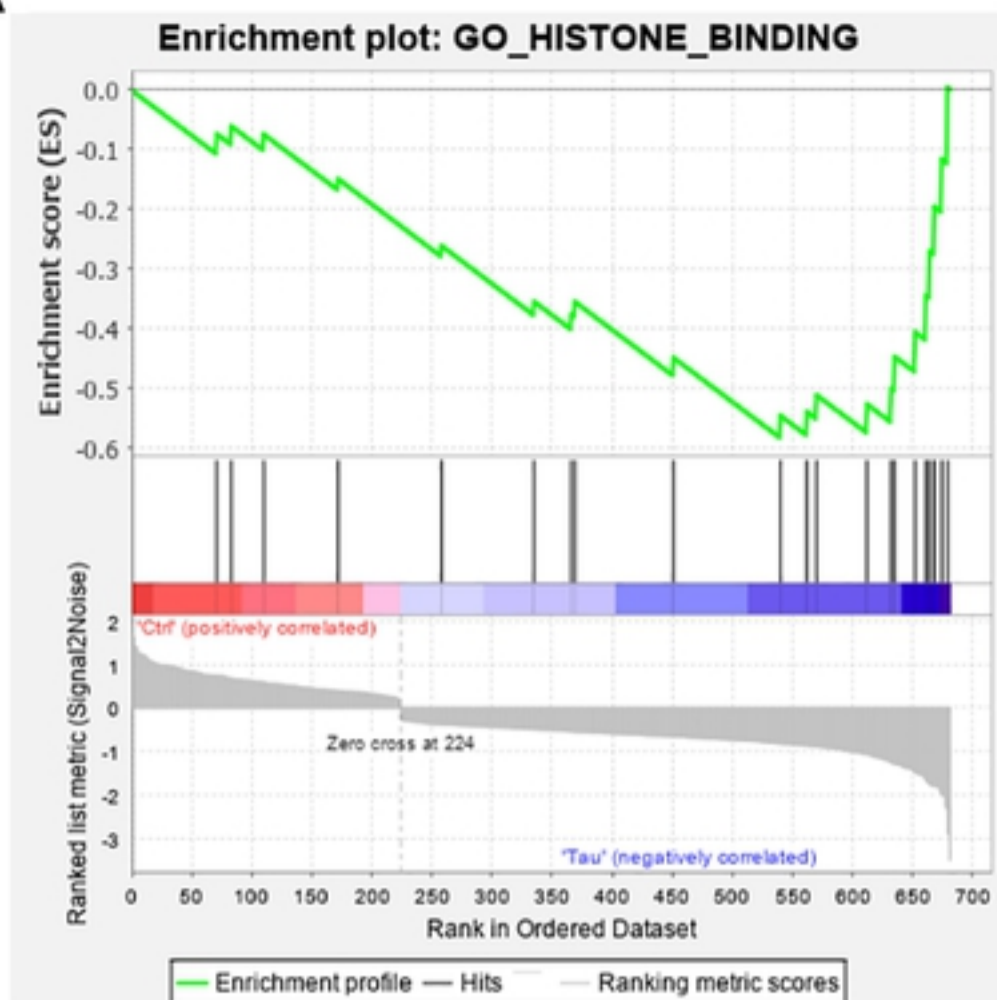
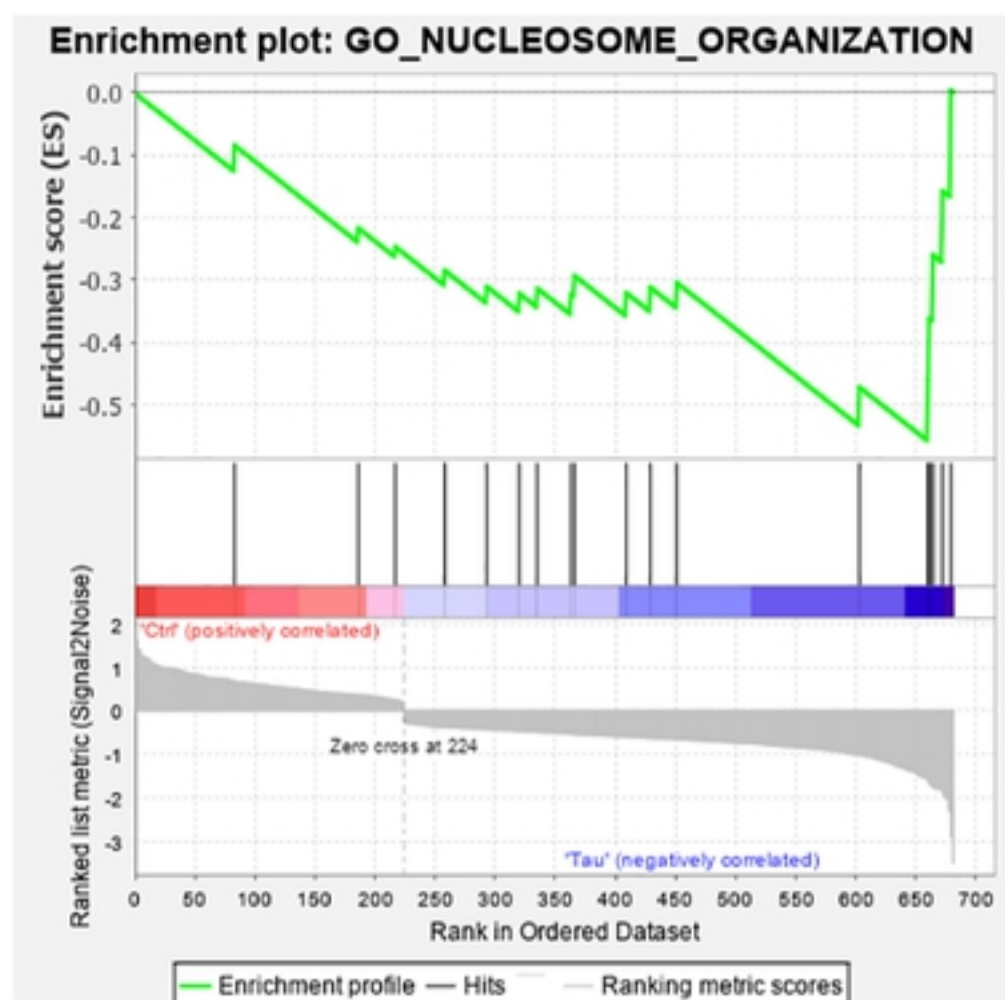


K

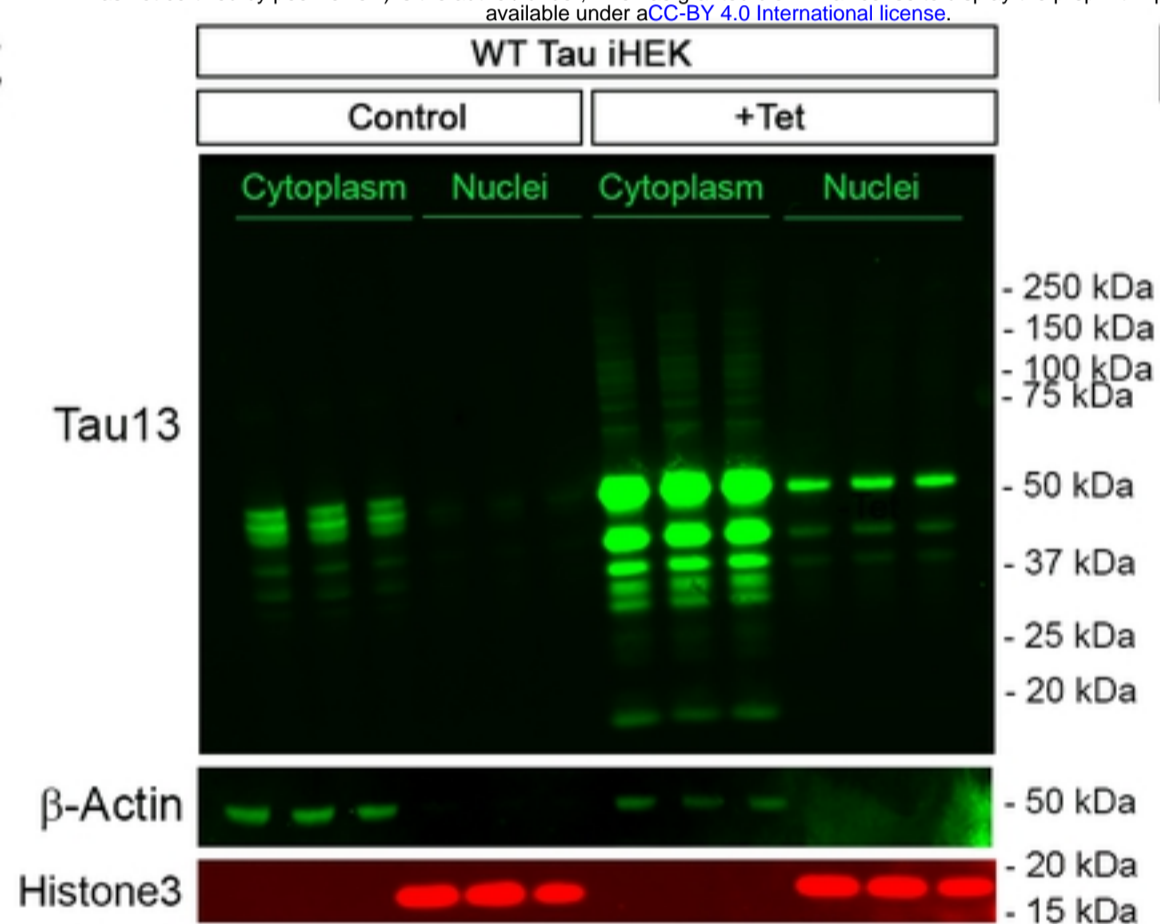
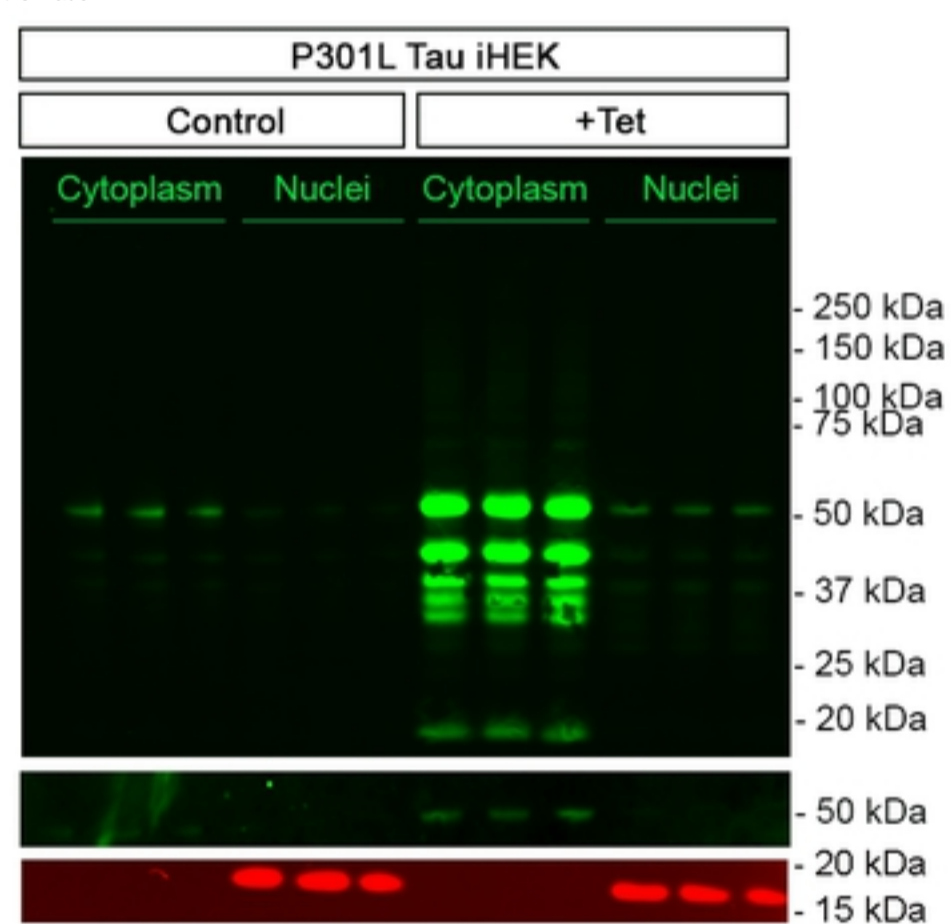
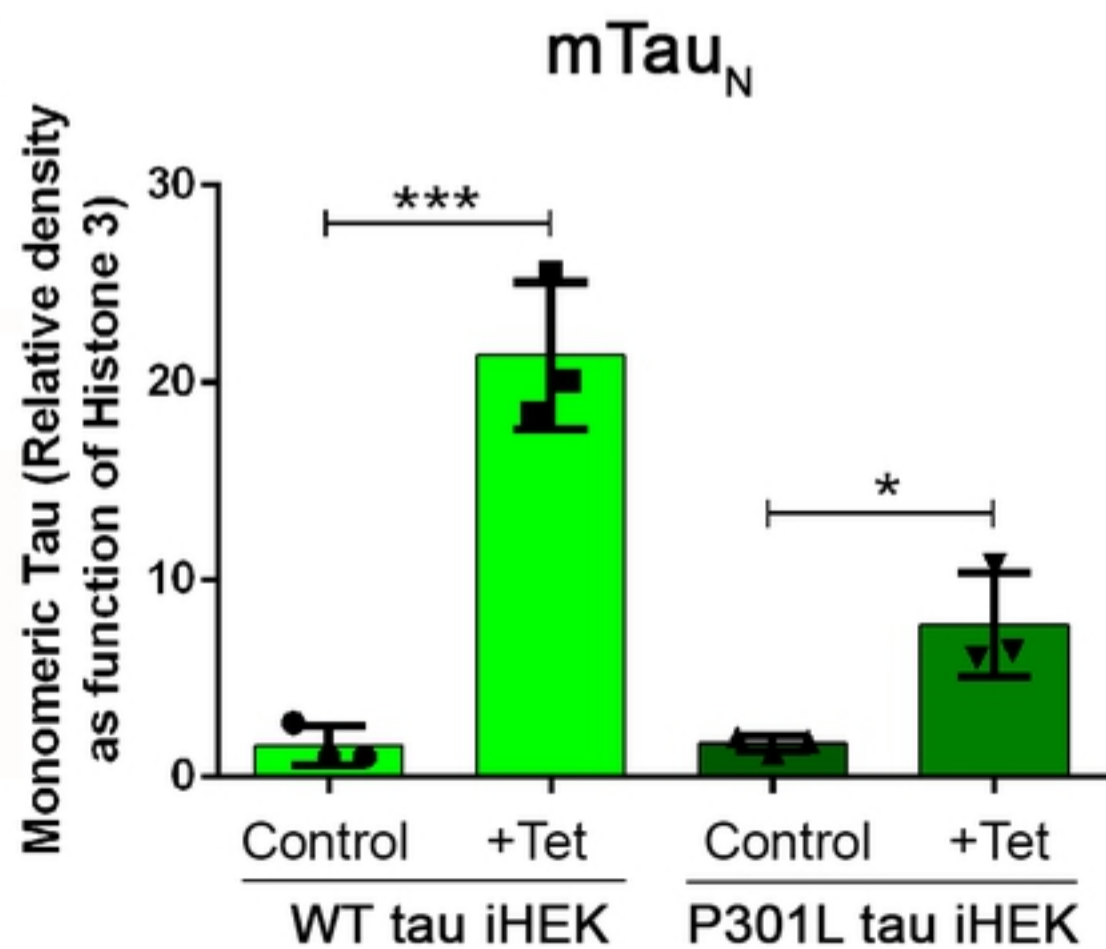
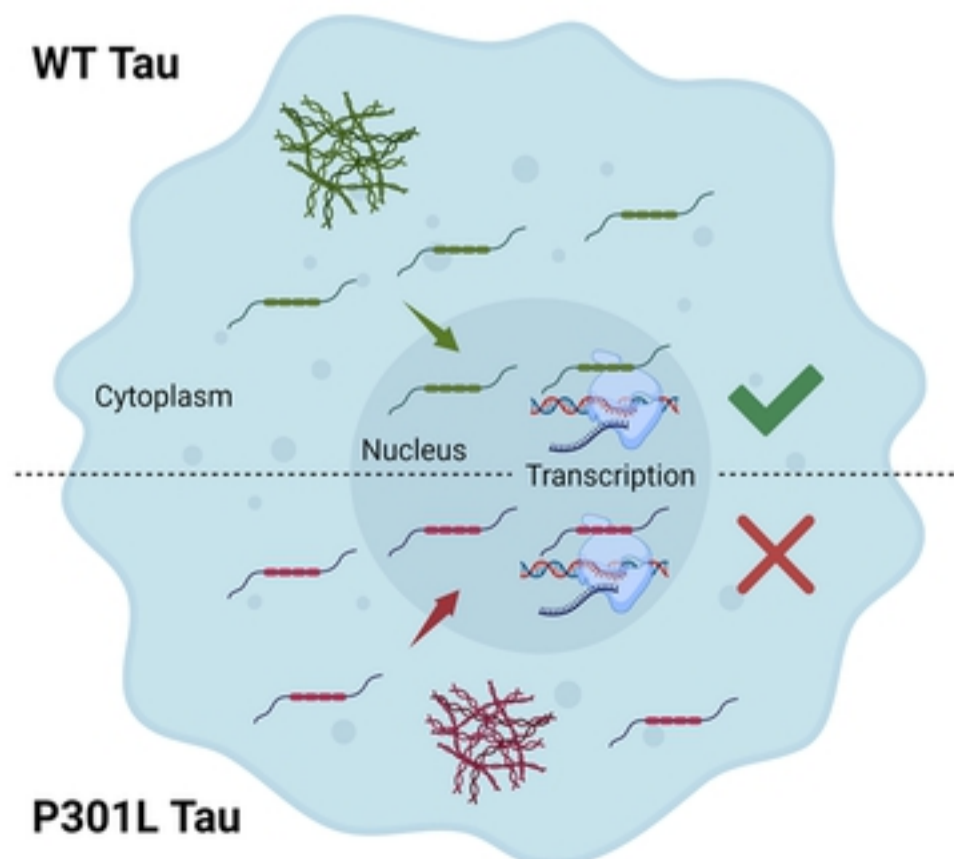


L

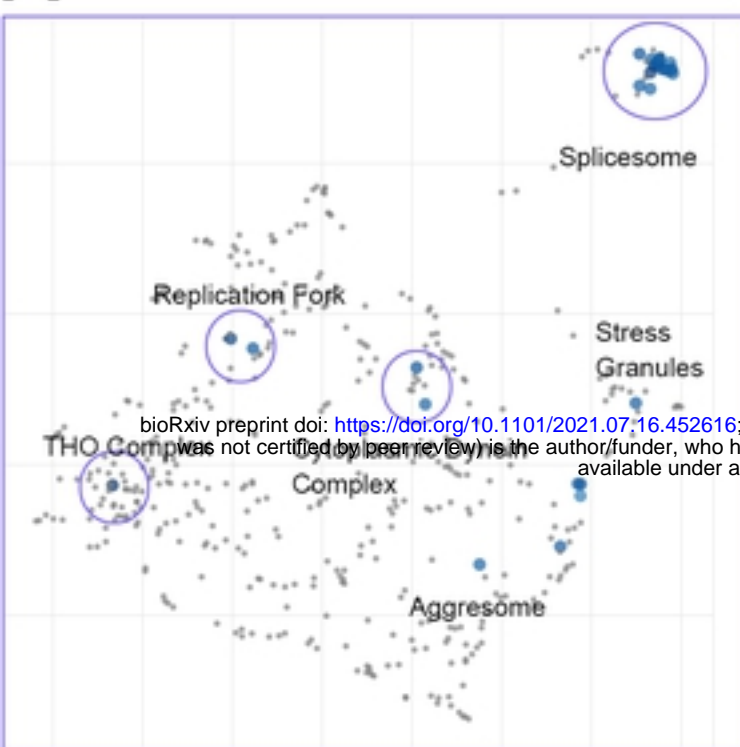


A**B**

bioRxiv preprint doi: <https://doi.org/10.1101/2021.07.16.452616>; this version posted July 16, 2021. The copyright holder for this preprint (which was not certified by peer review) is the author/funder, who has granted bioRxiv a license to display the preprint in perpetuity. It is made available under aCC-BY 4.0 International license.

C**D****E****F**

A

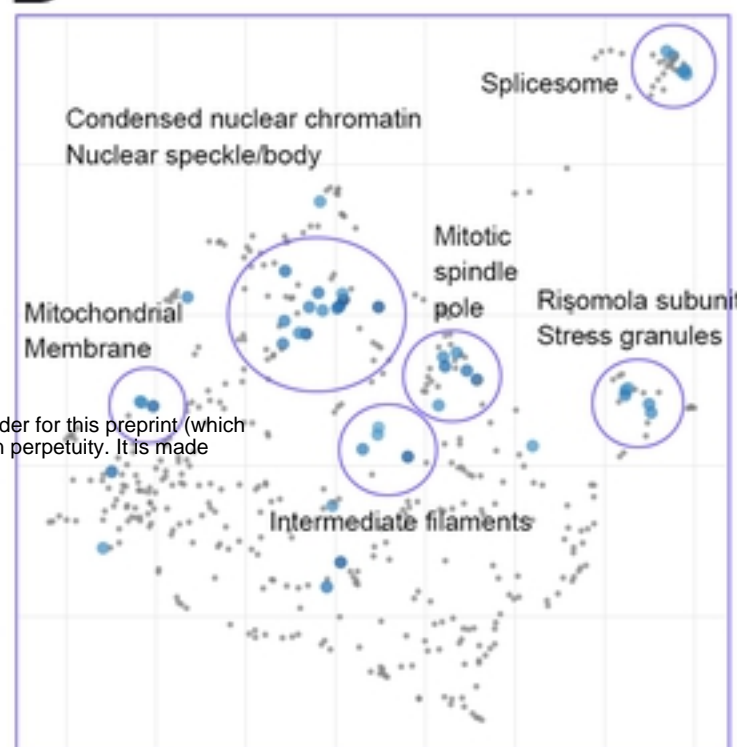


Scatterplot of gene clusters from lengthened mRNA precursors

Lengthened APAs Genes

WDR60	SLC16A1
SRSF7	TET1
DEGS1	
THOC2	
ARID4B	
HMG2	
HUWE1	
HNRNPF	
FASN	
JPT1	
EGR1	
SNRPE	
SLFN11	
GIGYF2	
TMA7	
PDIA6	
BAZ1B	
PRRC2C	
NASP	

B



Scatterplot of gene clusters from shortened mRNA precursors

Shortened APAs Genes

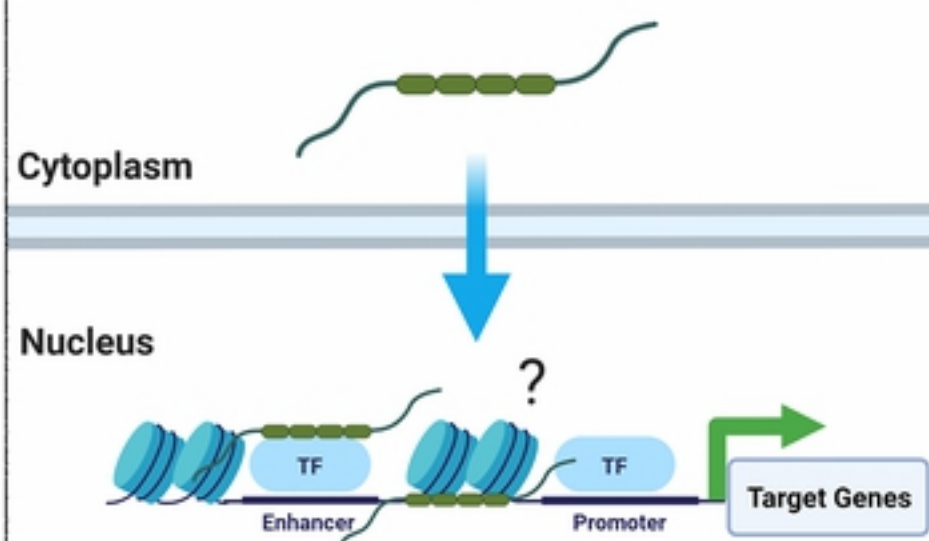
RAB13	SMC1A
NEFL	PMAIP1
EIF3A	H2AFY
UBE2G2	ID4
DBI	ARGLU1
HIST1H1E	NSRP1
PABPC1	DYNLL1
WDR5	KTN1
ACAT2	SRSF11
SHMT2	DSP
SRSF4	MARCKSL1
RPL22	PSIP1
GUSBP11	LUC7L3
CLK3	
CALM3	
MYO6	
IRS4	
SEN3-EIF4A1	
TOMM22	
RBM39	
ENTR1	

C

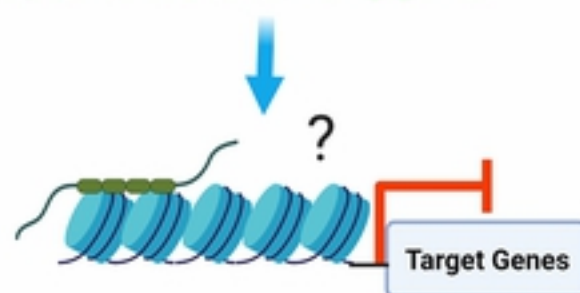
Nuclear Tau

Mechanism of action

Wild type Tau



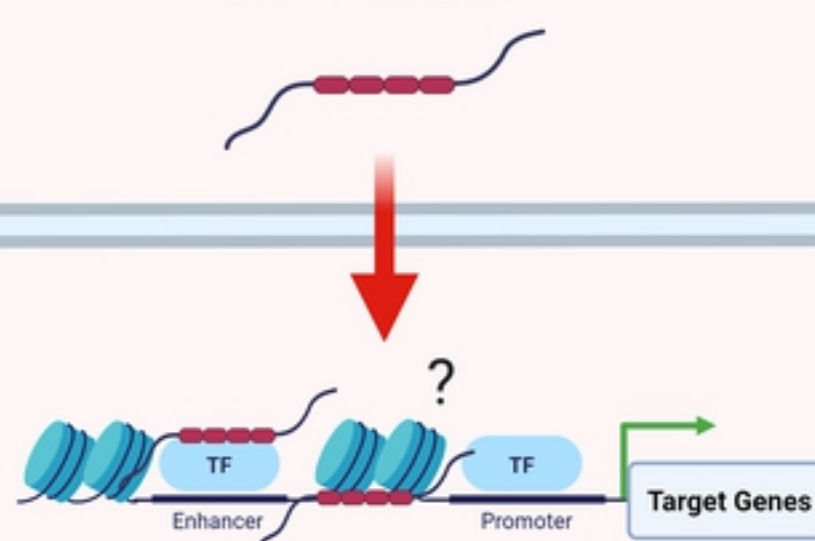
- Cytoskeleton organization/intacellular transport genes
- Microglia and macrophages activation genes
- Nuclear chromatin, nuclear body and specks genes
- RNA Binding Proteins associated genes
- Histone deacetylase binding
- Sequence-specific dsDNA binding genes



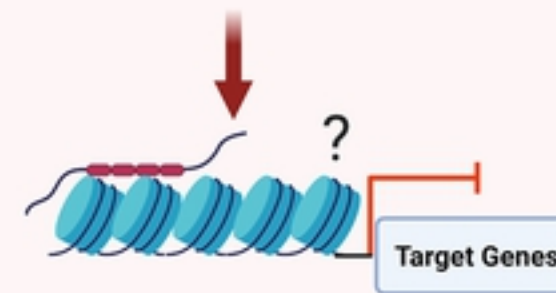
- Ubiquitin protein ligase binding
- Mitochondrial and Golgi apparatus genes

P301L Tau

FTDP-17 mutation



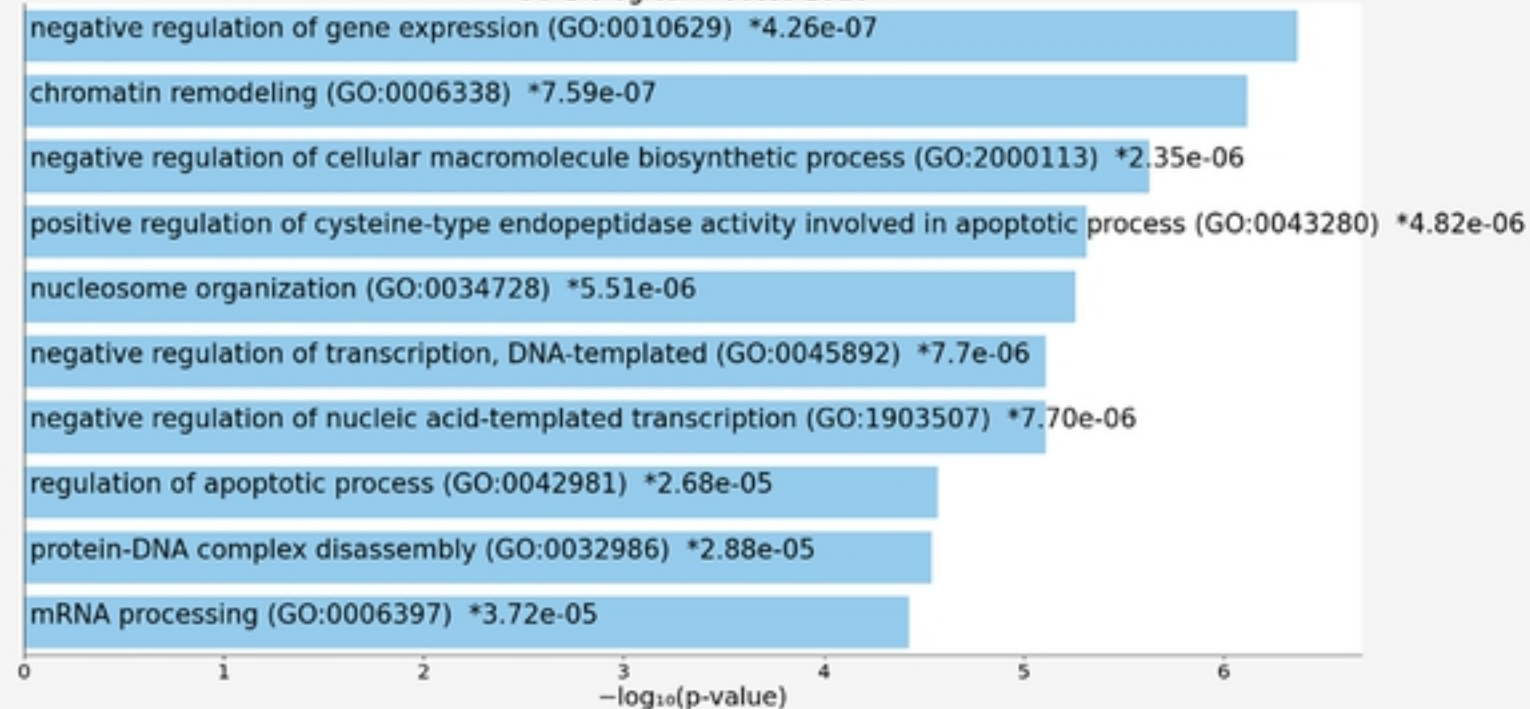
- Positive regulation of neuron death genes
- Response to reactive oxygen species genes
- Sequence-specific dsDNA binding genes
- Microtubule cytoskeleton genes
- Nuclear body and speck genes



- Ubiquitin ligase complex

A

GO Biological Process 2018

**B**

Genes with lengthed APAs

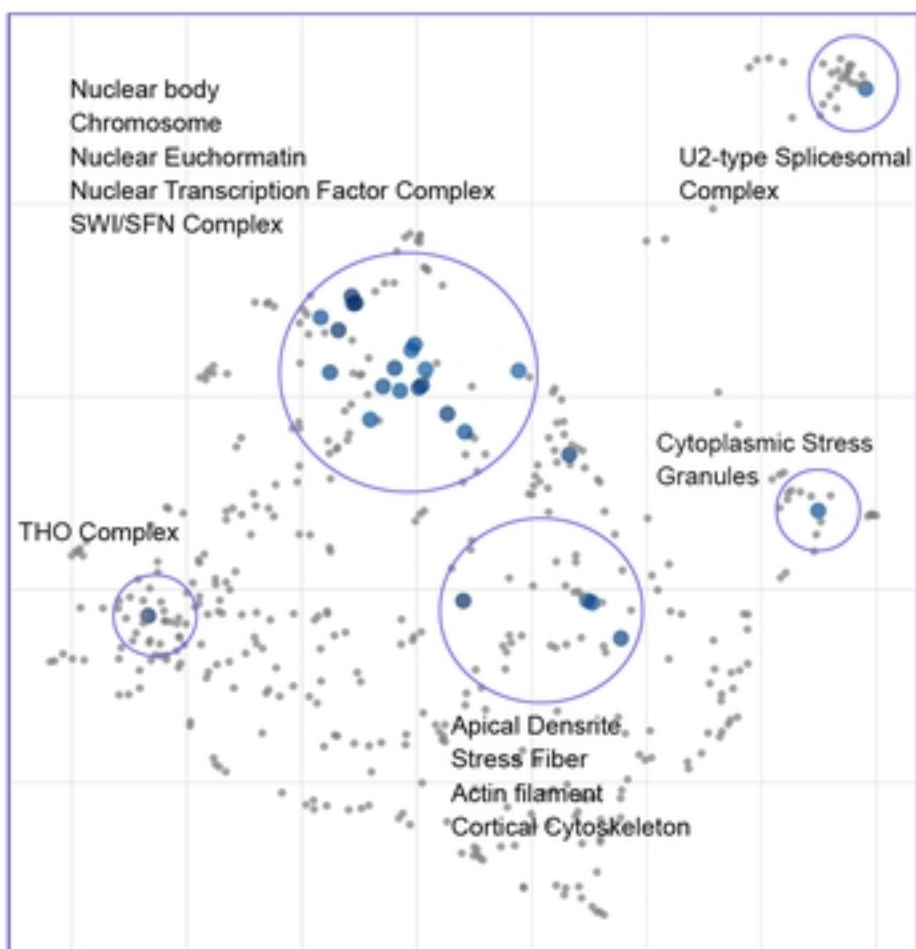
Negative control of gene expression: SMARCC2;POU2F1; PRMT2;CBX3;NONO;H3F3A; SMARCA2;POU3F3;SMARCA4; ILF3;SFPQ;BASP1; KAT6B;NCL;STC2;ID4;ANXA7;BIRC5; ZBTB7A;CNOT9

Chromatin remodelling: SMARCC2;CBX3;MYC;CHD1L;ANP32B; HMGB1;ARID1A;SMARCA2;SMARCA4

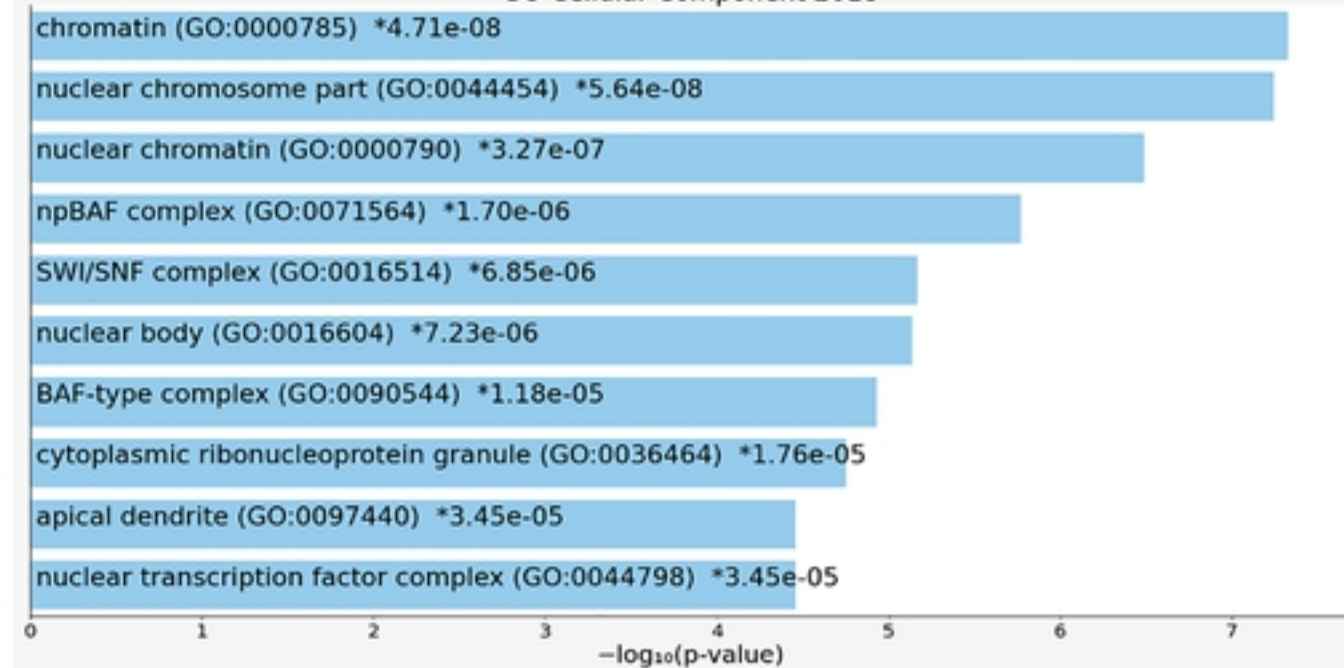
Nucleosome organization: SMARCC2;NASP;KAT6B;H3F3A; ANP32B;ARID1A;SMARCA4

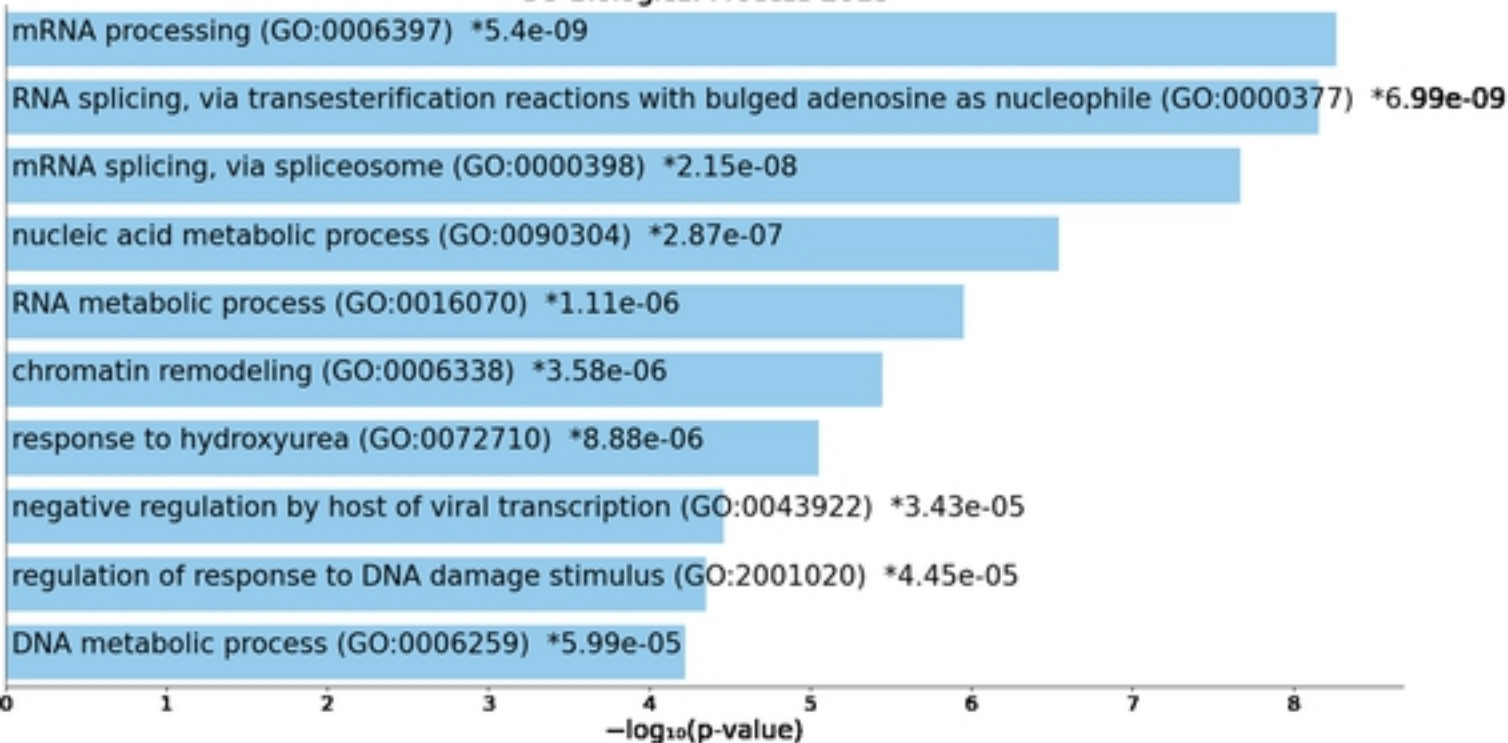
mRNA processing: SFPQ;NONO;HNRNPU;CDC5L;THOC3; THOC2;YBX1;PABPC1;SRSF6;ELAVL1;CTNBL1

Regulation of Transcription: ARID4B;NUCKS1;YBX1;HMGB1; PPP2R1A;BASP1;MYC;ZNF227;ZBTB7A;TRIM44;TCEAL9; SMARCC2;POU2F1;PRMT2;CDX2;CBX3;NONO;CDC5L; ARID1A;SMARCA2;POU3F3;SMARCA4;ILF3;SFPQ;KAT6B; ID4;BIRC5;ZNF711;PHIP;TCF3

C**D**

GO Cellular Component 2018



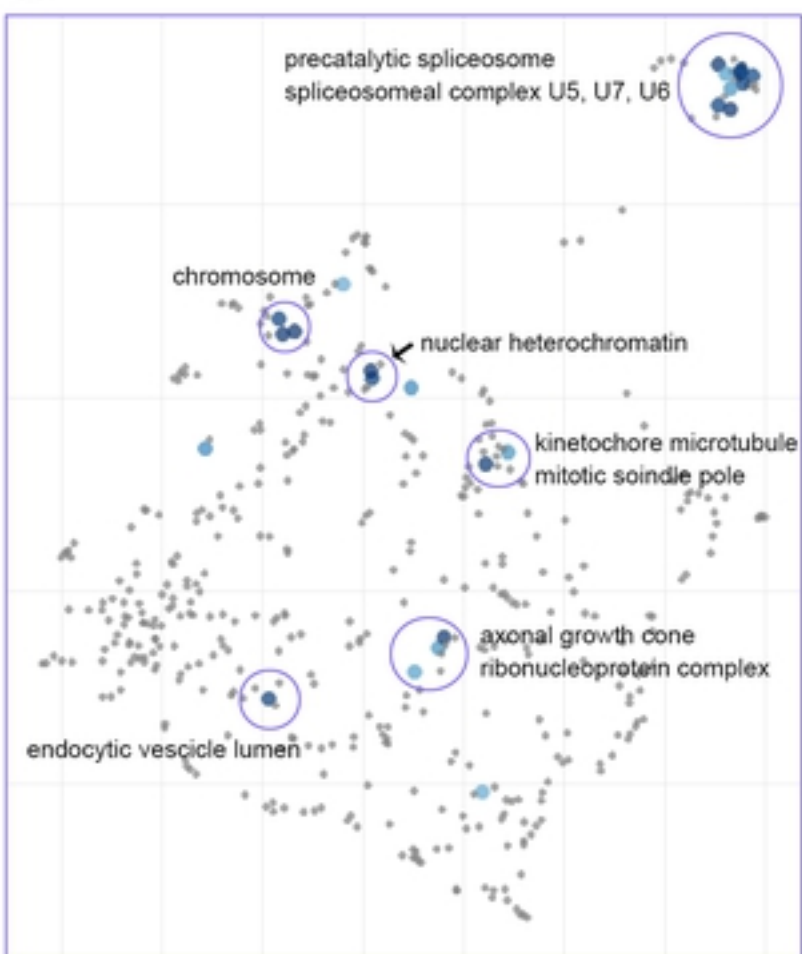
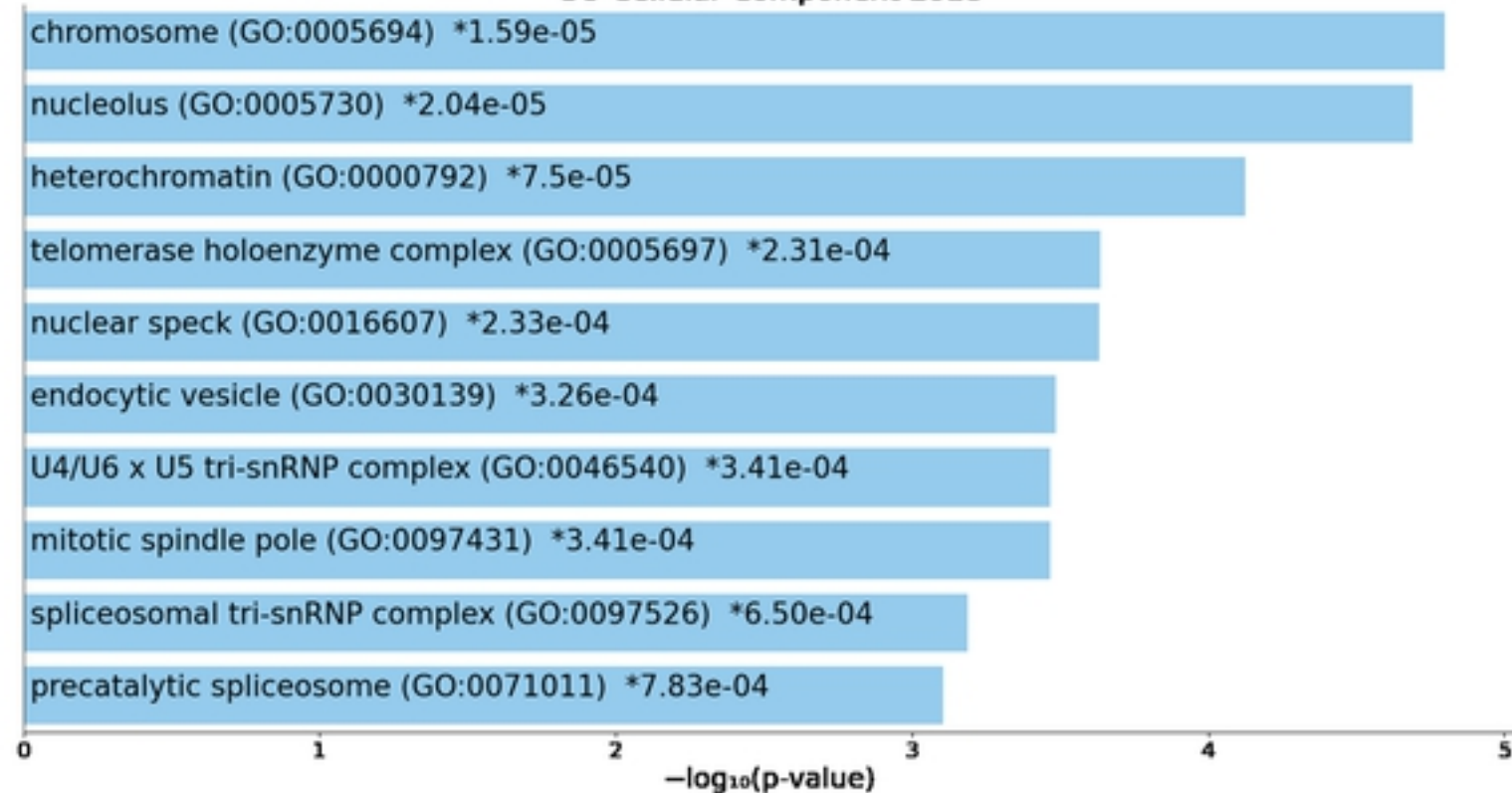
A**GO Biological Process 2018****B**

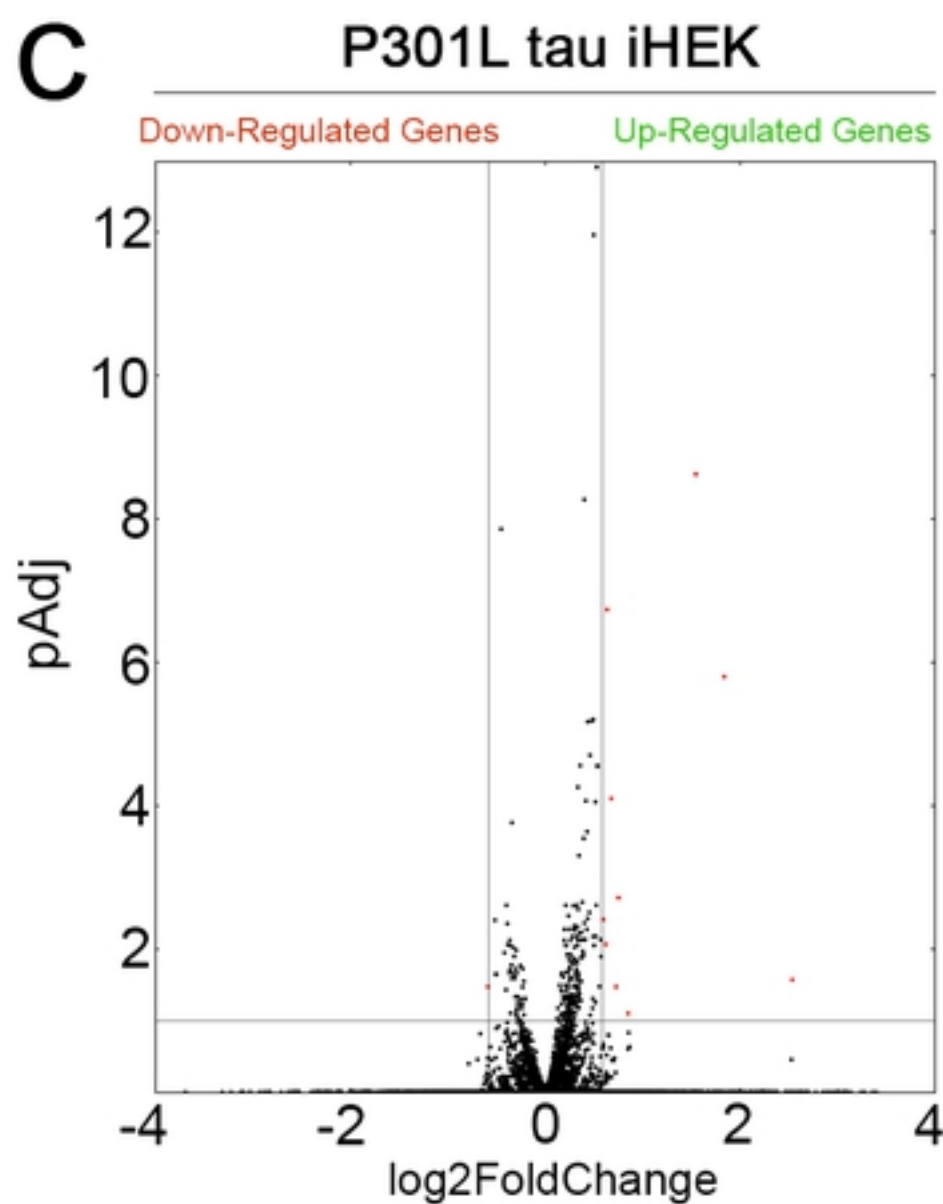
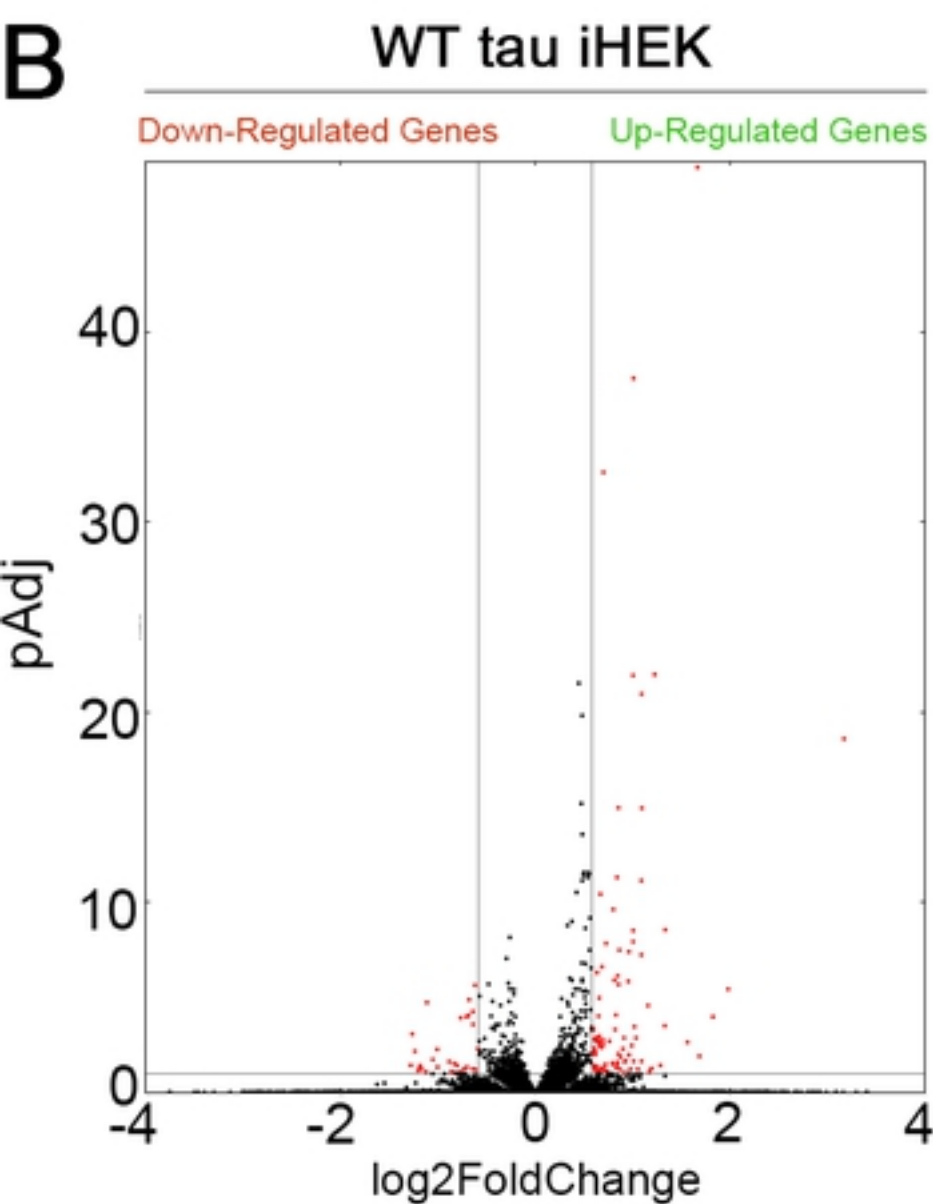
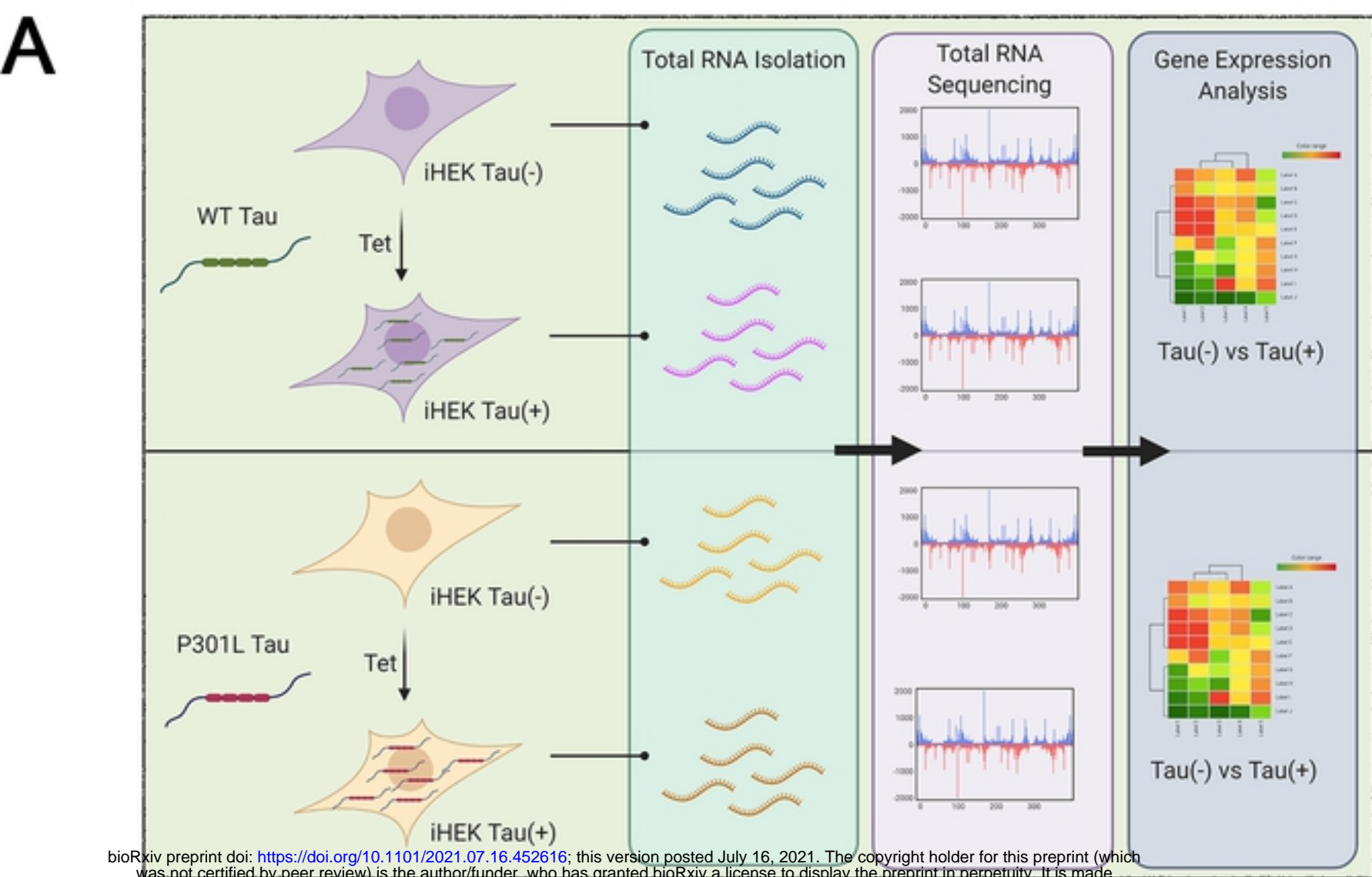
mRNA Processing: HNRNPA3;SRRT;PRPF4B;CCAR1;LSM8;SNRNP40;HNRNPK;ZMAT2;ZC3H11A;HNRNPF;PCBP2;SNRPE;HNRNPC

RNA Splicing: LSM8;HNRNPA3;SNRNP40;HNRNPK;ZMAT2;HNRNPF;PCBP2;SRRT;PRPF4B;SNRPE;HNRNPC;CCAR1

Chromatin remodelling: HDAC1;ATRX;ANP32E;HMGA2;HMGB3;HNRNPC;NUDT5

Regulation of response to DNA damage: BCLAF1;FMR1;USP1;HMGA2

C**D****GO Cellular Component 2018**



D Gene List Down- and Up-Regulated by WT Tau

Down (30 Genes)

DDIT4
NPIP811
PFDN2
TRIM33
STRIP1
MEGF9
KLHL11
MIRS48N
LYPD6
ORMDL1
UPF3A
OXCT1
STX6
ICAM5
IFRD1
STC2
ZMYM3
SNHG1
NCK1
SLC26A2
TRUB1
KCNQ2
KHDC4

SCIN
ID2
PSAT1
CCDC130
TSC22D3
UBE2T
BLZF1

Up (88 Genes)

DNAH14
C21orf59-TCP10L
SFSWAP
NRG3
ARHGAP11B
GTF2H2B
STRP2
RBM33
CPEB4
OTUD6B
KAT7
EPC2
IDA
GALNT6
ANP32E
MEF2A
MIRS48AC
CLCN3
PHF6
ZNF234
ZEB2
TARS
CDC73
RBM20

TACC1
IRS4
NBPFL1
NRGN
TNFRSF12A
PELP1
TUBA1A
SNAR-A11
SAP30BP
SMAD5
TUBA1B
TUBB2A
TUBB2B
BEX3
PRKG1
NOM1
GTF2H2C
SNAR-A2
PEA15
BMS1P20
NKAPD1
SUIPV3L1
LONRF3
TMOD3

SUPT5H
GIGYF1
FTSJ3
UBIAD1
RRP15
TRIM44
SNAR-A12
SEN2
UBE2Q2P2
BAZ2A
ARHGEP5
HIST1H1C
ARHGEP35
MAPT
SRRT
SDK1
TCHP
POLE3
DAAM1
UBE2E2
TRAF3BP1
N4BP2L2
DSE

MAP7
SUD53
CERK
TFRC
CARMIL1
CLU
HOOK3
ATP6V1D
HST2H2AC
USP36
DAGLB
HOXA6
TUBB2B
RHOQ
PHACTR1
TMEM178B
PANK4
ANKHD1-EIF4EBP3

E Gene List Down- and Up-Regulated by P301L Tau

Down (1 Gene)

DCAF12

Up (10 Genes)

NLGN1
FER
PLCB4
FOS
DDIT4
EGR1
RNAS-BSNS
ITPKC
TSPYL2
MAPT

WT tau

Up-regulated Gene Ontology

Biological Process

cytoskeleton-dependent intracellular transport (GO:0030705)
 microglial cell activation (GO:0001774)
 regulation of cytoskeleton organization (GO:0051493)
 mitochondrion distribution (GO:0048311)
 neurogenesis (GO:0022008)
 positive regulation of cell death (GO:0010942)
 maturation of 5.8S rRNA (GO:0000460)
 macrophage activation (GO:0042116)
 insulin receptor signaling pathway (GO:0008286)
 maturation of LSU-rRNA (GO:0000470)

Molecular Function

GTP binding (GO:0005525)
 purine ribonucleoside binding (GO:0032550)
 guanyl ribonucleotide binding (GO:0032561)
 RNA binding (GO:0003723)
 racemase and epimerase activity, acting on carbohydrates and derivatives (GO:0016857)
 double-stranded RNA binding (GO:0003725)
 histone deacetylase binding (GO:0042826)
 purine ribonucleoside triphosphate binding (GO:0035639)
 sequence-specific double-stranded DNA binding (GO:1990837)
 transcriptional repressor activity, RNA polymerase II transcription factor binding (GO:0001191)

Cellular Component

cytoskeleton (GO:0005856)
 polymeric cytoskeletal fiber (GO:0099513)
 nuclear chromatin (GO:0000790)
 microtubule cytoskeleton (GO:0015630)
 nuclear chromosome part (GO:0044454)
 microtubule (GO:0005874)
 preribosome, large subunit precursor (GO:0030687)
 nuclear speck (GO:0016607)
 cytoplasmic vesicle (GO:0031410)
 nuclear body (GO:0016604)

Down-regulated Gene Ontology

Biological Process

negative regulation of peptidyl-serine phosphorylation (GO:0033137)
 regulation of cell morphogenesis (GO:0022604)
 regulation of cellular component organization (GO:0051128)
 positive regulation of actin filament polymerization (GO:0030838)
 positive regulation of cytoskeleton organization (GO:0051495)
 regulation of anatomical structure morphogenesis (GO:0022603)
 regulation of peptidyl-serine phosphorylation (GO:0033135)
 positive regulation of megakaryocyte differentiation (GO:0045654)
 3'-phosphoadenosine 5'-phosphosulfate biosynthetic process (GO:0050428)
 signal complex assembly (GO:0007172)

Molecular Function

ubiquitin protein ligase binding (GO:0031625)
 ubiquitin-like protein ligase binding (GO:0044389)
 acetylcholine receptor regulator activity (GO:0030548)
 RNA polymerase II transcription factor binding (GO:0001085)
 cytoskeletal adaptor activity (GO:0008093)
 co-SMAD binding (GO:0070410)
 pseudouridine synthase activity (GO:0009982)
 oxalate transmembrane transporter activity (GO:0019531)
 sulfate transmembrane transporter activity (GO:0015116)
 transaminase activity (GO:0008483)

Cellular Component

axon initial segment (GO:0043194)
 node of Ranvier (GO:0033268)
 main axon (GO:0044304)
 SCF ubiquitin ligase complex (GO:0019005)
 coated vesicle (GO:0030135)
 ribosome (GO:0005840)
 perinuclear region of cytoplasm (GO:0048471)
 trans-Golgi network membrane (GO:0032588)
 clathrin-coated vesicle (GO:0030136)
 Golgi membrane (GO:0000139)

Supplemental Table 1. Up-Regulated Genes by WT Tau

Term	P-value	Adjusted P-value	Odds Ratio	Combined Score	Genes
cytoskeleton (GO:0005856)	1.73E-05	0.0077356 74	4.80769 2308	52.70303651	TUBA1B;SAP30BP;TUBB2B;TUBA1A;TMOD3;MAP7;TARS;TACC1;MAPT;CLU;RHOQ
polymeric cytoskeletal fiber (GO:0099513)	4.34E-04	0.0966945 62	6.17030 0288	47.77891745	TUBA1B;TUBB2B;TUBA1A;TUBB2A;MAPT;RHOQ
nuclear chromatin (GO:0000790)	8.81E-04	0.1309033 68	5.38986 705	37.91772839	MEF2A;ZEB2;ANP32E;SUDS3;HIST2H2AC;HIST1H1C
microtubule cytoskeleton (GO:0015630)	0.001616162	0.1802021 06	4.10028 1162	26.35538067	TUBA1B;TUBB2B;TUBA1A;TUBB2A;MAP7;TACC1;MAPT
nuclear chromosome part (GO:0044454)	0.001713127	0.1528109 38	4.05844 1558	25.84997914	MEF2A;ZEB2;POLE3;ANP32E;SUDS3;CDC73;HIST2H2AC
microtubule (GO:0005874)	0.00035899	0.1749798 1	5.41125 5411	32.71698914	TUBA1B;TUBB2B;TUBA1A;TUBB2A;MAPT
preribosome, large subunit precursor (GO:0030687)	0.00580801	0.3700532 18	17.4825 1748	90.00904291	RRP15;FTSJ3
nuclear speck (GO:0016607)	0.009908573	0.5524029 27	3.83906 6339	17.71481484	USP36;CARMIL1;GTF2H2C;BAZ2A;MAPT
cytoplasmic vesicle (GO:0031410)	0.015007567	0.7437083 22	4.22832 981	17.75560565	TFRC;ANP32E;CLCN3;RHOQ
nuclear body (GO:0016604)	0.019146203	0.8539206 72	2.57428 6555	10.18297877	USP36;CARMIL1;GTF2H2C;BAZ2A;MAPT;SUDS3;SENP2
axolemma (GO:0030673)	0.026114353	1	37.8787 8788	138.0784165	MAPT
nucleolus (GO:0005730)	0.029395392	1	2.35341 5815	8.300303054	USP36;NOM1;ZEB2;BAZ2A;PHF6;PELP1;FTSJ3
messenger ribonucleoprotein complex (GO:1990124)	0.030400721	1	32.4675 3247	113.4184725	CPEB4
spherical high-density lipoprotein particle (GO:0034366)	0.034668438	1	28.4090 9091	95.50924912	CLU
HFE-transferrin receptor complex (GO:1990712)	0.034668438	1	28.4090 9091	95.50924912	TFRC
Cdc73/Paf1 complex (GO:0016593)	0.034668438	0.9663827 14	28.4090 9091	95.50924912	CDC73
apical dendrite (GO:0097440)	0.034668438	0.9095366 72	28.4090 9091	95.50924912	CLU
chromatin silencing complex (GO:0005677)	0.034668438	0.8590068 57	28.4090 9091	95.50924912	BAZ2A
Swr1 complex (GO:0000812)	0.038917584	0.9135390 84	25.2525 2525	81.97750232	ANP32E
chromatin (GO:0000785)	0.041696789	0.9298384 01	3.07125 3071	9.758388048	MEF2A;ZEB2;HIST2H2AC;PELP1
preribosome (GO:0030684)	0.043179537	0.9170511 21	6.06060 6061	19.04477924	RRP15;FTSJ3
proton-transporting V-type ATPase complex (GO:0033176)	0.047360482	0.9601261 39	20.6611 5702	63.01584932	ATP6V1D
ribonucleoprotein granule (GO:0035770)	0.04848675	0.9402213 22	5.68181 8182	17.19582226	TUBA1A;MAPT

bioRxiv preprint doi: <https://doi.org/10.1101/2021.07.16.452610>; this version posted July 16, 2021. The copyright holder for this preprint (which was not certified by peer review) is the author/funder, who has granted bioRxiv a license to display the preprint in perpetuity. It is made available under aCC-BY 4.0 International license.

bioRxiv preprint doi: <https://doi.org/10.1101/2021.07.16.452616>; this version posted July 16, 2021. The copyright holder for this preprint (which was not certified by peer review) is the author/funder, who has granted bioRxiv a license to display the preprint in perpetuity. It is made available under aCC-BY 4.0 International license.

holo TFIIF complex (GO:0005675)	0.051554392	0.9580524 6	18.9393 9394	56.1575353	GTF2H2C
Sin3 complex (GO:0016580)	0.055730049	0.9942240 71	17.4825 1748	50.47615038	SUDS3
DNA-directed RNA polymerase II, holoenzyme (GO:0016591)	0.059760267	1	5.05050 5051	14.22936503	GTF2H2C;CDC73
cytoplasmic exosome (RNase complex) (GO:0000177)	0.064026913	1	15.1515 1515	41.64320855	SUPV3L1
keratin filament (GO:0045095)	0.064026913	1	15.1515 1515	41.64320855	TCHP
pericentriolar material (GO:0000242)	0.068148277	1	14.2045 4545	38.15439487	HOOK3
nuclear replisome (GO:0045095)	0.068148277	1	14.2045 4545	38.15439487	POLE3
Sin3-type complex (GO:0070822)	0.068148277	0.9804558 61	14.2045 4545	38.15439487	SUDS3
dendrite (GO:0030425)	0.06924185	0.9650582 79	3.17124 7357	8.46770561	MAPT;CLU;CPEB4
nuclear euchromatin (GO:0005719)	0.076337257	1	12.6262 6263	32.48224959	HIST1H1C
striated muscle thin filament (GO:0005865)	0.080405026	1	11.9617 2249	30.15165779	TMOD3
euchromatin (GO:0000791)	0.088487507	1	10.8225 1082	26.2434405	HIST1H1C
transcriptionally active chromatin (GO:0035327)	0.09250237	1	10.3305 7851	24.59215918	PELP1
histone acetyltransferase complex (GO:0000123)	0.09250237	1	10.3305 7851	24.59215918	KAT7
INO80-type complex (GO:0097346)	0.09250237	1	10.3305 7851	24.59215918	ANP32E
recycling endosome (GO:0055037)	0.09666912	1	3.81970 9702	8.924603778	TUBA1A;TFRC
contractile fiber (GO:0043292)	0.108387738	1	8.74125 8741	19.42342931	TMOD3
MLL1 complex (GO:0071339)	0.112315932	1	8.41750 8418	18.40437335	PELP1
myofibril (GO:0030016)	0.112315932	1	8.41750 8418	18.40437335	TMOD3
MLL1/2 complex (GO:0044665)	0.112315932	1	8.41750 8418	18.40437335	PELP1
main axon (GO:0044304)	0.135528342	1	6.88705 2342	13.76428715	MAPT
actin cytoskeleton (GO:0015629)	0.139839351	1	2.31910 9462	4.562293623	TMOD3;TARS;RHOQ
centrosome (GO:0005813)	0.145540984	1	1.97199 7634	3.800626224	TCHP;TRAF3IP1;HOOK3;ATP6V1 D
specific granule (GO:0042581)	0.1565438	1	2.84090 9091	5.268237029	CLCN3;ATP6V1D
contractile actin filament bundle (GO:0097517)	0.161851895	1	5.68181 8182	10.34700903	DAAM1

integral component of Golgi membrane (GO:0030173)	0.161851895	1	5.68181 8182	10.34700903	UBIAD1
stress fiber (GO:0001725)	0.161851895	1	5.68181 8182	10.34700903	DAAM1
heterochromatin (GO:0000792)	0.165547132	1	5.54323 7251	9.969508533	BAZ2A
cytoplasmic ribonucleoprotein granule (GO:0036464)	0.172060346	1	2.67379 6791	4.705641744	TUBA1A;MAPT
intermediate filament (GO:0005882)	0.183783091	1	4.94071 1462	8.369560635	TCHP
microtubule organizing center (GO:0005815)	0.184397492	1	1.79307 8716	3.031489277	TCHP;TRAF3IP1;HOOK3;ATP6V1D
cis-Golgi network (GO:0005801)	0.187382719	1	4.83558 9942	8.097689209	HOOK3
actomyosin (GO:0042641)	0.19058832	1	4.73484 8485	7.839282495	DAAM1
actin filament (GO:0005884)	0.215620364	1	4.13223 1405	6.339818153	RHOQ
perinuclear region of cytoplasm (GO:0048471)	0.232031019	1	1.80375 1804	2.635072538	GALNT6;TFRC;CLU
PML body (GO:0016605)	0.239531081	1	3.66568 915	5.238534082	SENP2
platelet alpha granule lumen (GO:0031093)	0.256167561	1	3.39213 0258	4.619821964	CLU
nucleoplasm part (GO:0044451)	0.266189763	1	1.67522 8948	2.217242288	GTF2H2C;KAT7;SUDS3
intermediate filament cytoskeleton (GO:0045111)	0.269217242	1	3.20102 4328	4.200501392	SAP30BP
lytic vacuole membrane (GO:0098852)	0.273570882	1	1.95083 8861	2.528666646	DAGLB;ATP6V1D
nuclear periphery (GO:0034399)	0.291511782	1	2.91375 2914	3.591709949	MAPT
clathrin-coated vesicle membrane (GO:0030665)	0.300859484	1	2.80583 6139	3.370123323	TFRC
phagocytic vesicle (GO:0045335)	0.307023439	1	2.73822 563	3.23338222	CLCN3
platelet alpha granule (GO:0031091)	0.328177166	1	2.52525 2525	2.813640594	CLU
specific granule membrane (GO:0035579)	0.331146544	1	2.49750 2498	2.76022545	ATP6V1D
clathrin-coated vesicle (GO:0030136)	0.357293708	1	2.27272 7273	2.33908437	TFRC
lysosomal membrane (GO:0005765)	0.367155241	1	1.56201 1871	1.565089849	DAGLB;ATP6V1D
nuclear chromosome, telomeric region (GO:0000784)	0.376929429	1	2.12404 418	2.072424172	CDC73
endocytic vesicle (GO:0030139)	0.379685681	1	2.10437 7104	2.037903041	CLCN3
chromosome, telomeric region (GO:0000781)	0.422181171	1	1.83284 4575	1.580499895	CDC73

bioRxiv preprint doi: <https://doi.org/10.1101/2021.07.16.452616>; this version posted July 16, 2021. The copyright holder for this preprint (which was not certified by peer review) is the author/funder, who has granted bioRxiv a license to display the preprint in perpetuity. It is made available under aCC-BY 4.0 International license.

microtubule organizing center part (GO:0044450)	0.427286491	1	1.80375 1804	1.533731156	HOOK3
late endosome (GO:0005770)	0.461796269	1	1.62337 6623	1.254271854	CLCN3
axon (GO:0030424)	0.464181054	1	1.61186 3314	1.237073825	MAPT
RNA polymerase II transcription factor complex (GO:0090575)	0.478271942	1	1.54607 2975	1.140345997	GTF2H2C
lysosome (GO:0005764)	0.557038143	1	1.07712 193	0.630247266	DAGLB;ATP6V1D
Golgi membrane (GO:0000139)	0.582354922	1	1.02838 3381	0.556021375	GALNT6;DSE
early endosome (GO:0005769)	0.626341943	1	1.02375 1024	0.478970947	CLCN3
early subcompartment (GO:0098791)	0.626341943	1	1.02375 6669	0.478970947	GALNT6;DSE
mitochondrion (GO:0005739)	0.667382777	1	0.88605 3518	0.358312528	TCHP;SUPV3L1;MAPT;CLU
mitochondrial matrix (GO:0005759)	0.745573163	1	0.73789 8465	0.216648473	SUPV3L1
secretory granule lumen (GO:0034774)	0.755626978	1	0.71694 8666	0.20089435	CLU
integral component of plasma membrane (GO:0005887)	0.96056947	1	0.46604 1136	0.018748356	TFRC;NRG3;CLCN3

bioRxiv preprint doi: <https://doi.org/10.1101/2021.07.16.452616>; this version posted July 16, 2021. The copyright holder for this preprint (which was not certified by peer review) is the author/funder, who has granted bioRxiv a license to display the preprint in perpetuity. It is made available under aCC-BY 4.0 International license.

Supplemental Table 2 - Down-Regulated Genes by WT Tau

Term	P-value	Adjusted P-value	Odds Ratio	Combined Score	Genes
axon initial segment (GO:0043194)	0.013421829	1	74.07407407	319.3239135	KCNQ2
node of Ranvier (GO:0033268)	0.017856968	1	55.55555556	223.6311935	KCNQ2
main axon (GO:0044304)	0.048367756	1	20.2020202	61.19034096	KCNQ2
SCF ubiquitin ligase complex (GO:0019005)	0.077961385	1	12.34567901	31.50051407	KLHL11
coated vesicle (GO:0030135)	0.101264667	1	9.389671362	21.5025138	STX6
ribosome (GO:0005840)	0.108009525	1	8.771929825	19.52224439	NCK1
perinuclear region of cytoplasm (GO:0048471)	0.109697823	1	3.527336861	7.795505317	STC2;STX6
trans-Golgi network membrane (GO:0032588)	0.128027161	1	7.843137255	16.62774289	STX6
clathrin-coated vesicle (GO:0030136)	0.139709564	1	6.666666667	13.1212637	STX6
Golgi membrane (GO:0000139)	0.141642689	1	3.016591252	5.895769726	STX6;BLZF1
Golgi subcompartment (GO:0098791)	0.160952725	1	2.783576896	5.084605682	STX6;BLZF1
mitochondrion (GO:0005739)	0.197703841	1	1.949317739	3.159815052	TRUB1;OXCT1;PFDN2
cullin-RING ubiquitin ligase complex (GO:0031461)	0.238857152	1	3.683241252	5.273994836	KLHL11
trans-Golgi network (GO:0005802)	0.243455603	1	3.603603604	5.091245694	STX6
nucleolus (GO:0005730)	0.269438542	1	1.972386588	2.586617276	UBE2T;UPF3A
early endosome (GO:0005769)	0.284737465	1	3.003003003	3.772335434	STX6
endoplasmic reticulum lumen (GO:0005788)	0.335058182	1	2.469135802	2.699879222	STC2
mitochondrial matrix (GO:0005759)	0.37245128	1	2.164502165	2.13776849	OXCT1
integral component of plasma membrane (GO:0005887)	0.377736622	1	1.367053999	1.330906484	SLC26A2;KCNQ2;ICAM5

bioRxiv preprint doi: <https://doi.org/10.1101/2021.07.16.452616>; this version posted July 16, 2021. The copyright holder for this preprint (which was not certified by peer review) is the author/funder, who has granted bioRxiv a license to display the preprint in perpetuity. It is made available under aCC-BY 4.0 International license.

Supplemental Table 3. Up-Regulated Genes by P301L Tau

Term	P-value	Adjusted P-value	Odds Ratio	Combined Score	Genes
axolemma (GO:0030673)	0.002996578	1	333.3333333	1936.761417	MAPT
dendrite (GO:0030425)	0.004890312	1	18.60465116	98.98603085	NLGN1;MAPT
filopodium tip (GO:0032433)	0.004989818	0.741819593	200	1060.071173	NLGN1
spanning component of membrane (GO:0089717)	0.005487568	0.611863795	181.8181818	946.412758	NLGN1
nuclear speck (GO:0016607)	0.009082553	0.810163748	13.51351351	63.53243152	ITPKC;MAPT
microtubule cytoskeleton (GO:0015630)	0.015239427	1	10.30927835	43.13267377	FER;MAPT
main axon (GO:0044304)	0.016381548	1	60.60606061	249.1878617	MAPT
cytoskeleton (GO:0005856)	0.026441482	1	7.692307692	27.94477859	FER;MAPT
filopodium (GO:0040175)	0.029604508	1	333.3333333	117.3275068	NLGN1
nuclear body (GO:0016604)	0.036393121	1	6.472491909	21.44579618	ITPKC;MAPT
nuclear periphery (GO:0034399)	0.038330884	1	25.64102564	83.62818815	MAPT
ribonucleoprotein granule (GO:0035770)	0.039296097	1	25	80.91575164	MAPT
axon (GO:0030424)	0.068319537	1	14.18439716	38.0646738	MAPT
RNA polymerase II transcription factor complex (GO:0090575)	0.07113123	1	13.60544218	35.9622965	FOS
cytoplasmic ribonucleoprotein granule (GO:0036464)	0.081838782	1	11.76470588	29.44710636	MAPT
microtubule (GO:0005874)	0.100196316	1	9.523809524	21.91070345	MAPT
polymeric cytoskeletal fiber (GO:0099513)	0.105186383	1	9.049773756	20.38028436	MAPT
nuclear chromatin (GO:0000790)	0.119561652	1	7.90513834	16.78990615	FER
actin cytoskeleton (GO:0015629)	0.137676093	1	6.802721088	13.48878577	FER
chromatin (GO:0000785)	0.138551081	1	6.756756757	13.35483925	FER
nuclear chromosome part (GO:0044454)	0.179622583	1	5.102040816	8.759680555	FER
nucleolus (GO:0005730)	0.291015997	1	2.958579882	3.652003078	TSPYL2
mitochondrion (GO:0005739)	0.409477333	1	1.949317739	1.740494599	MAPT
integral component of plasma membrane (GO:0005887)	0.532245452	1	1.367053999	0.862133316	NLGN1

bioRxiv preprint doi: <https://doi.org/10.1101/2021.07.16.452616>; this version posted July 16, 2021. The copyright holder for this preprint (which was not certified by peer review) is the author/funder, who has granted bioRxiv a license to display the preprint in perpetuity. It is made available under aCC-BY 4.0 International license.

Supplemental Figure 4. Down-Regulated Genes by P301L Tau

Term	P-value	Adjusted P-value	Odds Ratio	Combined Score	Genes
Cul4-RING E3 ubiquitin ligase complex (GO:0080008)	0.0018	0.80278471	555.5556	3511.104	DCAF12
cullin-RING ubiquitin ligase complex (GO:0031461)	0.00905	1	110.4972	519.8896	DCAF12
centrosome (GO:0005813)	0.02305	1	43.38395	163.5617	DCAF12
microtubule organizing center (GO:0005815)	0.02535	1	39.44773	144.9697	DCAF12

bioRxiv preprint doi: <https://doi.org/10.1101/2021.07.16.452616>; this version posted July 16, 2021. The copyright holder for this preprint (which was not certified by peer review) is the author/funder, who has granted bioRxiv a license to display the preprint in perpetuity. It is made available under aCC-BY 4.0 International license.